MODELING OF COLLECTION OF NON-SPHERICAL PARTICLE ASSEMBLIES BY LIQUID DROPLETS UNDER POTENTIAL FLOW CONDITIONS

A Thesis Submitted to
the Graduate School of Engineering and Sciences of
İzmir Institute of Technology
in Partial Fulfillment of the Requirements for the Degree of

MASTER OF SCIENCE

in Chemical Engineering

by
İlker SELVİ

March 2006
İZMİR

We approve the thesis of **İlker SELVİ**

Date of Signature

.....
Yrd. Doç Dr. Fuat DOYMAZ
Supervisor
Department of Chemical Engineering
İzmir Institute of Technology

27 March 2006

.....
Doç Dr. Mehmet POLAT
Co-Supervisor
Department of Chemical Engineering
İzmir Institute of Technology

27 March 2006

.....
Yrd. Doç Dr. Şebnem ELÇİ
Department of Civil Engineering
İzmir Institute of Technology

27 March 2006

.....
Doç Dr. Hürriyet POLAT
Department of Chemistry
İzmir Institute of Technology

27 March 2006

.....
Prf. Doç Dr. Devrim BALKÖSE
Head of Department
İzmir Institute of Technology

27 March 2006

.....
Doç Dr. Semahat ÖZDEMİR
Head of the Graduate School

ACKNOWLEDGMENTS

I would like to thank Dr. Fuat Doymaz for guiding me at every stage in this study, and Dr. Mehmet Polat for offering me this title. Thanks to Şebnem Elçi and Hürriyet Polat for corrections on my thesis writing. Many thanks go to family for their patience and support they have given me throughout my life. Thanks to Ertuğrul Anadolu for being my best friend and for providing me technical support.

ABSTRACT

A model, which explains the collection of non-spherical particle assemblies by liquid droplets, was constructed. The system was investigated under potential flow conditions. It was possible to generate the streamlines around the particles and droplets via potential flow theory. Therefore, the complexity coming from eddies and vorticity was eliminated. Non-spherical particles and agglomerated particles were modeled using equivalent diameter assumption due to the boundary layer, rotation, and oscillation behaviors of the particles. Collection probability was calculated as a function of three different collection mechanisms: collision, adhesion, and engulfment. The interaction forces between particles and droplets were divided into two groups as external and internal forces. The gravitational force and the drag force due to the uniform flow rate caused collection mechanisms. Van der Waals and Electrostatic interactions were investigated in order to explain adhesion and wetting mechanisms. Through simulations, we have found that particle and droplet diameters were the most influencing parameters on the collision mechanism. The engulfment possibility could be increased by adding surfactant to the liquid solution. The results of this model showed similarities with the other models in the literature, as well as with that of the experimental studies.

ÖZET

Küresel olmayan tanecik gruplarının damlacıklar tarafından toplanmasının modelleme çalışması yapılmıştır. Sistem potansiyel akım koşulları altında incelenmiştir. Taneciklerin ve damlacıkların etrafındaki akım çizgileri potansiyel akım teorisi yardımı ile çizilmiştir. Aynı zamanda, potansiyel akım teorisi girdap ve türbülans dolayısı ile oluşacak karmaşık durumların yok sayılması açısından önemlidir. Taneciklerin salınım ve kendi eksenleri etrafında dönmeleri hesaba katılarak eşdeğer çap varsayımı yapılmıştır. Eşdeğer çap varsayımı küresel olmayan tanecik grupları için önemli bir yaklaşımdır. Taneciklerin toplanması çarpışma, yapışma ve içine alma olmak üzere üç alt işlem olarak incelenmiştir. Tanecik ve damlacıkların etkileşimlerine sebep olan kuvvetler dış ve iç olmak üzere iki gruba ayrılmıştır. Hava akımı sayesinde oluşan sürükleyici kuvvet ve yerçekimi kuvveti dış kuvvet grubunu oluştururken; Van der Waals ve elektriksel kuvvetler iç kuvvetleri oluşturmaktadır. Bilgisayar simülasyonu sayesinde çarpışma olasılığı hesaplanmış; tanecik ve damlacık sayısının ve boyutunun bu olasılık değeri üzerinde etkili olduğu bulunmuştur. Damlacıklara yüzey kimyasallarının eklenmesi ile damlacıkların tozları içine alma olasılığının arttırılabileceği görülmüştür. Elde edilen model, literatürde yer alan diğer modeller ve deneysel bulgular ile benzerlik göstermektedir.

TABLE OF CONTENTS

LIST OF FIGURES

LIST OF TABLES

Table **Page**

NOMENCLATURE

A	:	Area (m^2).
A_{ij}	:	Hamaker Constant for interaction of particles i and j.(J).
a	:	Half of the distance between source and sink in doublet (m).
C_C	:	Cunningham Correction Factor.
C_D	:	Drag Coefficient.
C_i	:	Electrolyte concentration of the solution.
d	:	Diameter of particle (m).
d_e	:	Equivalent diameter (m).
E	:	Electrical field strength.
e_0	:	Electronic charge (1.602189×10^{-19} C).
F	:	Faraday constant (9.64845×10^4 C/mole).
F_D	:	Drag Force (N).
F_{VdW}	:	Van der Waals force (N).
F_{El}	:	Electrostatic force (N).
G_H	:	Free energy of electrical double layer system when surfaces are separated by a distance H.
G_∞	:	Free energy of electrical double layer system when surfaces are separated by a distance of infinity.
g	:	Gravitational acceleration.
H	:	Length of gap separating of two macroscopic bodies (m).
h	:	Planck's constant (6.626176×10^{-34} J.s).
K	:	İmpaction Parameter.
k	:	Boltzmann constant (1.380662×10^{23} J/K).
M_i	:	Molecular weight of component i (kg/mole).
m	:	Volumetric flow rate of fluid per unit length in source and sink (m^2/s); mass (kg).
N_A	:	Avagadro's number.
$n_{cap.}$	:	Number of captured particles.
$n_{tot.}$	:	Number of total particles in control volume.
P	:	Pressure (bar).

$P_{collection}$: Collection probability.

$P_{collision}$: Collision probability.

$P_{adhesion}$: Adhesion probability.

$P_{engulfment}$: Engulfment probability.

R : Gas constant.

Re : Reynolds number.

r : Radius (m).

q : Total charge of particle.

T : Absolute temperature (K).

t : time (s).

U : Uniform flow rate (m/s).

u_i : Velocity component of the particle.

V_{el} : Electrostatic energy of interaction between macroscopic bodies.

$V_{0,i}$: Frequency of the electron for molecule i (Hz).

υ_x : x component of velocity in rectangular coordinates (m/s).

υ_y : y component of velocity in rectangular coordinates (m/s).

υ_z : z component of velocity in rectangular and cylindrical coordinates (m/s).

υ_r : r component of velocity in cylindrical and spherical coordinates (m/s).

υ_θ : θ component of velocity in cylindrical and spherical coordinates (m/s).

υ_Φ : Φ component of velocity in spherical coordinates (m/s).

z_i : Valance of the counter ion.

α : Angle (radian).

$\alpha_{0,i}$: Static polarizability of molecule i (C^2m^2/J).

β_{ij} : London parameter for molecules i and j ($J.m^6$).

γ : Surface tension.

ε : Relative permittivity of water.

ε_0 : Permittivity of vacuum ($8.854x10^{-12}$ $C^2/J.m$).

$\varepsilon_j(i\zeta)$: Dielectric constant of material j as a function of the imaginary electromagnetic frequency.

η : Collection Efficiency.

θ : Angle (radian); Contac angle.

κ : Reciprocal thickness of the double layer (1/m).

λ : Molecular mean free path in the gas (m).

μ : Viscosity of Fluid (kg/.m.s).

μ_i : Dipole moment of molecule i (C.m).

ρ : Density (kg/m^3); charge (C).

σ_i : Surface charge density of material I (C/m^2).

τ : Relaxation of particle (1/s).

Ψ : Stream function (m^2); surface potential (volts).

Φ : Velocity potential (m^2/s).

Φ_K : Energy of Keesom between atom and molecules (J).

Φ_D : Energy of Debye between atom and molecules (J).

Φ_L : Energy of London between atom and molecules (J).

Φ_{VdW} : Energy of Van der Waals between atom and molecules (J).

CHAPTER 1

INTRODUCTION

Particles are everywhere! The matter is that what kinds of particles are harmful and which methods can be used in order to suppress them. The particles that settle down on our furniture may be a problem, or the particles in our shoes when we walk on the beach may also be a problem. However, these problems can be easily solved because their solution is straight forward. The major concerns are the particles that are invisible and harmful. These invisible and so small particles can go into our respiratory system and cause some serious health consequences such as pnömokonyoz.

Coal mines are places where respirable dusts are major problems for mine workers. Particles smaller than 10μm can easily diffuse and deposit in the respiratory system of the workers (Polat H., Polat M. and Gürgen 2000). There have been many dust removal methods since this problem were realized. These dust removal methods, their efficiencies and cost of them are tabulated in Table 1.1. (DHHS 2003).

Table 1.1. Dust removal methods, efficiencies and cost.

Dust Control Method	**Effectiveness**	**Cost**
Dilution Ventilation	Moderate	High
Displacement Ventilation	Moderate to high	Moderate
Wetting by sprays	Moderate	Low
Airborne capture by sprays	Low	Low
Airborne capture by high pressure sprays	Moderate	Moderate
Foam	Moderate	High
Dust collectors	Moderate to high	Moderate to high
Reducing generated dust	Low to moderate	Moderate
Enclosure with spray	Low to moderate	Moderate
Dust avoidance	Moderate	Low to Moderate

Collection of dust particles by liquid droplets is effective and cheap method as it is seen in the Table 1.1. However, the theory behind this mechanism is not easy as it is seen. Collection of dust particles by liquid droplets is a field that concerns fluid dynamics, Quantum mechanics, analytical methods, colloid science and physical chemistry. Simple and complex experiments can be carried out in order to understand the behavior of the collection mechanism. Models on the collection mechanisms are useful for design parameters on scrubbers and many air cleaning equipments.

The collection mechanism can be divided into three parts. These parts are collision, adhesion and engulfment (Chander et al. 1991). Theory must be analyzed in order to understand their main collection mechanisms. The particles are suspended in air with the liquid droplets. Flow conditions are very effective on the collection mechanism. Particles and droplets would be suspended in turbulent, laminar or transitional flow. There exists vorticity also. These real phenomena make the system complex because determination of pathways of the particles and droplets under non-ideal conditions is very challenging. Potential flow assumption must be done in order to reduce the complexity. The most important result of potential flow is that there is no vorticity because flow assumed as irrotational, incompressible and inviscid (Munson et al. 2002), (Leal 1992). The most famous result of the potential flow theory is streamlines around objects. Streamlines around the droplets will be the path ways of the particle if there is no force acting on the bodies. However, particles exit their pathways while traveling through the streamlines by the forces acting up on them. The particle will be collected by the liquid droplets by these forces. This collection can be by sedimentation, inertia impaction, interception, electrostatic interaction and diffusion (WEB_1 2006).

In order to model the system, the forces acting on it must be analyzed properly. Two kinds of forces will affect the bodies. These are called external and internal forces. External forces deal with the external conditions not depending on particle whereas the internal forces depend on the particle's physical, chemical and electrochemical properties.

Gravitational force is the most important and famous force acting on the system. Gravitational force is an external force which causes sedimentation. The other and important force is drag force due to the flow conditions. Determinations of drag coefficients are usually complex for many systems such as air crafts, cars and particles. It is an important parameter that depends on the shape of particle and Reynolds number

(Concha and Almedra 1979a), (Concha and Almedra 1979b), (Concha and Barrientos 1982), (Concha and Barrientos 1986), (Concha and Christiansen 1986). Van der Waals interaction is the most famous internal interaction. This interaction is due to the electrical dipole moment of the particles (Polat H. and Polat M. 2000a), (Israelachvili 1992). The other important and complex internal force between bodies is electrostatic interactions. Electrostatic interactions are hard to quantify due to the particle's changeable charge density and non-uniform electric field of the environment (Polat 1999), (Polat H. and Polat M. 2000b), (Park and Young 2005).

There are several modeling studies in the literature in order to understand the collection mechanisms of particles by liquid droplets. The difference of this study is about the shape consideration. Particles and droplets are considered as rigid spheres in the other modeling studies. Particles and droplets do not have uniform geometries in reality. Though (Polat et al. 2002), (Wu and Manasseh 1998) various assumptions used to simplify behaviors of non-spherical agglomerated particles in this study such particles' behaviors were modeled taking a different approach.

The model was developed using various theories. In the following chapters, these theories were described first, then assumptions stated and finally though simulation using Matlab version 6, results were generated. Comparisons of the model performance with other's available in the literature were given for several cases.

CHAPTER 2

THEORY

2.1. Potential Flow Theory

Potential Flow Theory is one of the most important theories in the fluid mechanics. This theory was suggested in order to express the flow characteristics such as velocity, pressure drop. Flow is considered as inviscid, incompressible and irrotational. This type of flow fields are governed by Laplace's equation in potential flow theory. It was supported by many important terms and equations. In this study, potential flow assumption is utilized in order to reduce the complexity from the boundary layer separation. Pathways of particles around droplets are also determined by potential flow streamlines. First, some basic fluid mechanics terms will be mentioned before going into details about this theory.

2.1.1. The Continuity Equation

The continuity equation is commonly referred to as the differential equation of conservation of mass. The continuity equation for rectangular coordinates is:

$$\frac{\partial \rho}{\partial t} + \frac{\partial (\rho v_x)}{\partial x} + \frac{\partial (\rho v_y)}{\partial y} + \frac{\partial (\rho v_z)}{\partial z} = 0 \tag{2.1}$$

The continuity equation for cylindrical coordinates is:

$$\frac{\partial \rho}{\partial t} + \frac{1}{r}\frac{\partial (r\rho v_r)}{\partial r} + \frac{1}{r}\frac{\partial (\rho v_\theta)}{\partial \theta} + \frac{\partial (\rho v_z)}{\partial z} = 0 \tag{2.2}$$

The continuity equation for spherical coordinates is:

$$\frac{\partial \rho}{\partial t} + \frac{1}{r^2}\frac{\partial (r^2 \rho v_r)}{\partial r} + \frac{1}{r\sin\theta}\frac{\partial (\rho \sin\theta v_\theta)}{\partial \theta} + \frac{1}{r\sin\theta}\frac{\partial (\rho v_\phi)}{\partial \phi} = 0 \tag{2.3}$$

Parameters appear in the above equations are defined in the Nomenclature list given on page xi, thus in subsequent chapters the reader is referred to this page for parameters' definition appear in equations.

2.1.2. Incompressible Flow

Flow is incompressible when there is no density change with time and position. If these conditions are applied to the continuity equations the incompressible flow expressions can be obtained for rectangular, cylindrical and spherical coordinates. The incompressible flow can be expressed as in general:

$$\nabla . V = 0 \tag{2.4}$$

The incompressible flow in rectangular coordinates is defined as:

$$\frac{\partial v_x}{\partial x} + \frac{\partial v_y}{\partial y} + \frac{\partial v_z}{\partial z} = 0 \tag{2.5}$$

The incompressible flow in cylindrical coordinates is defined as:

$$\frac{1}{r}\frac{\partial (r v_r)}{\partial r} + \frac{1}{r}\frac{\partial (v_\theta)}{\partial \theta} + \frac{\partial (v_z)}{\partial z} = 0 \tag{2.6}$$

The incompressible flow in spherical coordinates is defined as:

$$\frac{1}{r^2}\frac{\partial (r^2 v_r)}{\partial r} + \frac{1}{r\sin\theta}\frac{\partial (\sin\theta v_\theta)}{\partial \theta} + \frac{1}{r\sin\theta}\frac{\partial (v_\phi)}{\partial \phi} = 0 \tag{2.7}$$

2.1.3. Irrotational Flow

The meaning of irrotational fluid is there is no rotation of fluid element. The vorticity of fluid equals to zero. Angular motion and deformation will be neglected. The irrotational fluid can be explained as:

$$\nabla \times V = 0 \tag{2.8}$$

The irrotational flow in rectangular coordinates is defined as:

$$\left(\frac{\partial v_z}{\partial y} - \frac{\partial v_y}{\partial z}\right)\hat{x} + \left(\frac{\partial v_x}{\partial z} - \frac{\partial v_z}{\partial x}\right)\hat{y} + \left(\frac{\partial v_y}{\partial x} - \frac{\partial v_x}{\partial y}\right)\hat{z} = 0 \tag{2.9}$$

The irrotational flow in cylindrical coordinates is defined as:

$$\left(\frac{1}{r}\frac{\partial v_z}{\partial \theta} - \frac{\partial v_\theta}{\partial z}\right)\hat{r} + \left(\frac{\partial v_r}{\partial z} - \frac{\partial v_z}{\partial r}\right)\hat{\theta} + \left(\frac{1}{r}\frac{\partial (r v_\theta)}{\partial r} - \frac{1}{r}\frac{\partial v_r}{\partial \theta}\right)\hat{z} = 0 \tag{2.10}$$

The irrotational flow in spherical coordinates is defined as:

$$\left(\frac{1}{r\sin\theta}\frac{\partial (v_\phi \sin\theta)}{\partial \theta} - \frac{1}{r\sin\theta}\frac{\partial v_\theta}{\partial \phi}\right)\hat{r} + \left(\frac{1}{r\sin\theta}\frac{\partial v_r}{\partial \phi} - \frac{1}{r}\frac{\partial (r v_\phi)}{\partial r}\right)\hat{\theta} + \left(\frac{1}{r}\frac{\partial (r v_\theta)}{\partial r} - \frac{1}{r}\frac{\partial v_r}{\partial \theta}\right)\hat{\phi} = 0 \tag{2.11}$$

2.1.4. Inviscid Flow

If there is no shear stress in the flow field, this type of fluid is termed as inviscid flow. Inviscid fluid can be expressed as nonviscid or frictionless fluid. All the components of the shear stresses will be zero.

2.1.5. Stream Function

Flow field and its properties are affected due to type of the fluid. The inviscid, incompressible and irrotational flow could be explained by equations given in previous sections. However, the flow must be considered as two-dimensional in order to express the flow field and determine the velocity components.. Therefore, there will be two velocity components. A new function that called as stream function Ψ is defined in order to express the velocity components of two-dimensional flow field. Velocity components in terms of stream function for rectangular coordinates:

$$v_x = \frac{\partial \psi}{\partial y} \qquad v_y = -\frac{\partial \psi}{\partial x} \tag{2.12}$$

Velocity components in terms of stream function for cylindrical coordinates:

$$v_r = \frac{1}{r}\frac{\partial \psi}{\partial \theta} \qquad v_\theta = -\frac{\partial \psi}{\partial r} \tag{2.13}$$

Velocity components in terms of stream function for spherical coordinates:

$$v_r = \frac{1}{r}\frac{\partial \psi}{\partial \theta} \qquad v_\theta = -\frac{\partial \psi}{\partial r} \tag{2.14}$$

2.1.6. Velocity Potential

Velocity potential is a definition that expresses the velocity components of the flow field as a scalar function. Velocity potential is a consequence of irrotational flow while stream function is a consequence of continuity equation. Furthermore, velocity potential can be expressed in three-dimensional form while stream function expresses in two dimensional. For rectangular coordinates the velocity potential is:

$$v_x = \frac{\partial \phi}{\partial x} \quad v_y = \frac{\partial \phi}{\partial y} \quad v_z = \frac{\partial \phi}{\partial z} \tag{2.15}$$

For cylindrical coordinates the velocity potential is:

$$v_r = \frac{\partial \phi}{\partial r} \quad v_\theta = \frac{1}{r}\frac{\partial \phi}{\partial \theta} \quad v_z = \frac{\partial \phi}{\partial z} \tag{2.16}$$

For spherical coordinates the velocity potential is:

$$v_r = \frac{\partial \phi}{\partial r} \quad v_\theta = \frac{1}{r}\frac{\partial \phi}{\partial \theta} \quad v_\phi = \frac{1}{r\sin\theta}\frac{\partial \phi}{\partial \phi} \tag{2.17}$$

2.1.7. Potential Flow

Inviscid, irrotational and incompressible flow field are governed by Laplace's equation and this theory is called as potential flow theory. For incompressible fluid the continuity equation is express by Eq. 2.4. If velocity vector is replaced by velocity potential, the result will be:

$$\nabla^2 \phi = 0 \tag{2.18}$$

where, $\nabla^2() = \nabla.\nabla()$ is the Laplacian operator. The solution of Eq. 2.18 for different geometries will give the potential flow field of fluid.

In this study, potential flow field around a sphere is investigated. Potential flow stream lines are defined around droplets in order to define the pathways of the particles. Theory and definitions stated above will be used in order to draw stream lines around the objects. Uniform flow, source, sink and doublet must be expressed in terms of above definitions and equations in order to draw stream lines around a cylinder and sphere.

2.1.8. Uniform Flow

Uniform flow is the simplest possible potential flow. In uniform flow, stream lines due to the flow are all straight and parallel to each other and also the magnitude of velocity is constant. Two different uniform flows are illustrated in Figure 2.1. Uniform flow can be expressed in terms of velocity potential and stream function. There is only x component of velocity in Figure 2.1.(a); v_x = U and $v_y = 0$.

$$\frac{\partial \phi}{\partial x} = U \quad \frac{\partial \phi}{\partial y} = 0 \tag{2.19}$$

Then the velocity potential for uniform flow in x direction will be:

$$\phi = Ux \tag{2.20}$$

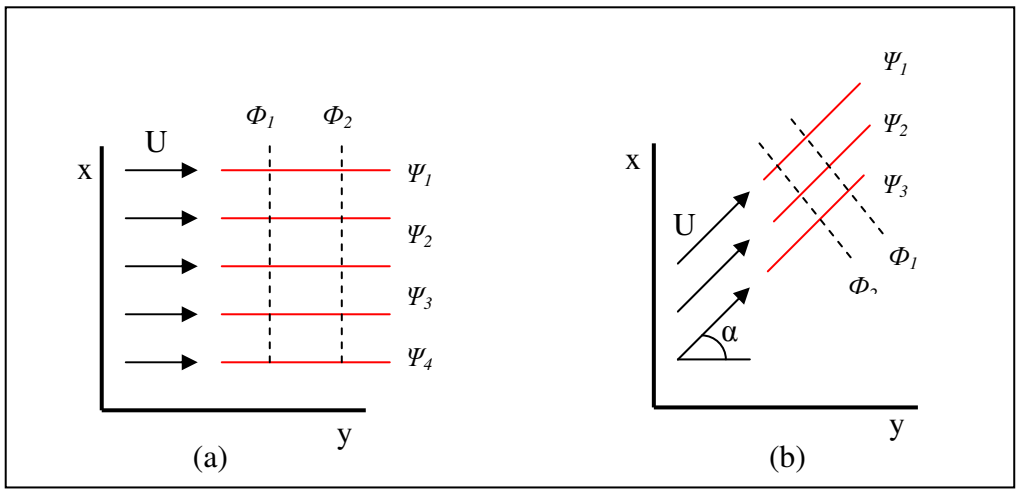

Figure 2.1. Uniform flow (a) in x direction ,(b) in arbitrary direction.

The stream function can be calculated similarly;

$$\frac{\partial \psi}{\partial y} = U \qquad \frac{\partial \psi}{\partial x} = 0 \tag{2.21}$$

Then the stream function for uniform flow in x direction will be:

$$\psi = Uy \tag{2.22}$$

There is a uniform flow in Figure 2.1.(b) in arbitrary direction. The velocity components will be v_x = U.cosα and v_y = U.sinα.

$$\frac{\partial \phi}{\partial x} = U\cos\alpha \qquad \frac{\partial \phi}{\partial y} = U\sin\alpha \tag{2.23}$$

Then the velocity potential for uniform flow arbitrary direction will be:

$$\phi = U(x\cos\alpha + y\sin\alpha) \tag{2.24}$$

The stream function can be calculated similarly;

$$\frac{\partial \psi}{\partial y} = U\cos\alpha \qquad \frac{\partial \psi}{\partial x} = U\sin\alpha \tag{2.25}$$

Then the stream function for uniform flow arbitrary direction will be:

$$\psi = U(y\cos\alpha - x\sin\alpha) \tag{2.26}$$

2.1.9. Source and Sink

A fluid that is outward from a hole flowing through a line perpendicular to the x-y plane is called as source. However; a fluid that is inward from a hole flowing through a line perpendicular to the *x*-*y* plane is called as sink. Schematic illustration of source and sink is illustrated in Figure 2.1. Assume that the volumetric flow rate of the fluid per unit length, *m*, is constant for both source and sink. "*m*" will be greater than zero for source whereas it will be smaller than zero for sink. Volumetric flow rate could be calculated from conservation of mass:

$$m = (2\pi r)v_r \tag{2.27}$$

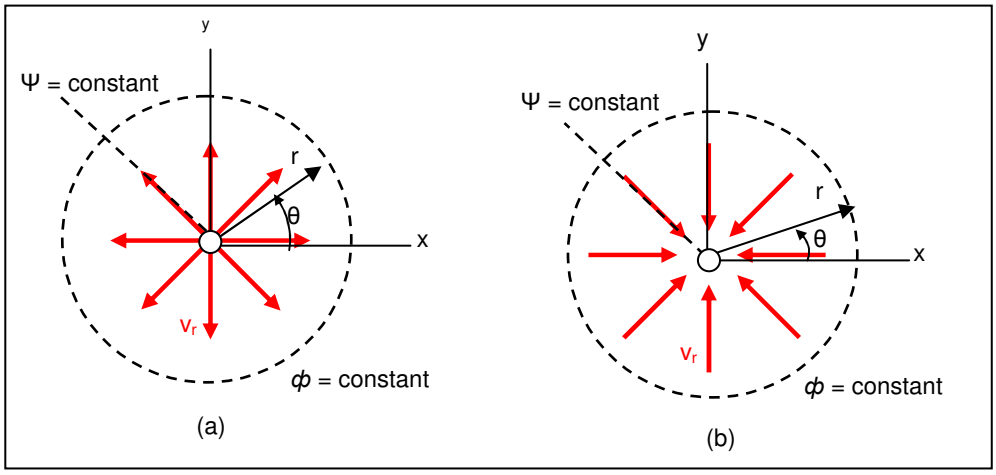

Figure 2.2. (a) Streamline pattern for a source, (b) Streamline pattern for a sink.

$$v_r = \frac{m}{2\pi.r} \tag{2.28}$$

There is only radial component of the velocity vector, v_θ. Stream function and velocity potential can be calculated by using Equations 2.1.13 and 2.1.16 respectively. The stream function of source and sink are:

$$\psi = \frac{m}{2\pi}\theta \qquad \psi = -\frac{m}{2\pi}\theta \tag{2.29}$$

The velocity potential of source and sink are:

$$\psi = \frac{m}{2\pi}\ln r \qquad \psi = -\frac{m}{2\pi}\ln r \tag{2.30}$$

2.1.10. Doublet

If a source and a sink are combined with each other, a doublet will be formed. The streamlines outward from the source will be collected by sink. Doublet is the preliminary step to draw the streamlines around spheres and other geometries. Schematic illustration of doublet is shown in Figure2.3. The stream function of doublet is:

$$\psi_{doublet} = \psi_{source} + \psi_{\sin k}$$
$$\psi_{doublet} = \psi = \frac{m}{2\pi}\theta_2 - \frac{m}{2\pi}\theta_1 = -\frac{m}{2\pi}(\theta_1 - \theta_2) \tag{2.31}$$

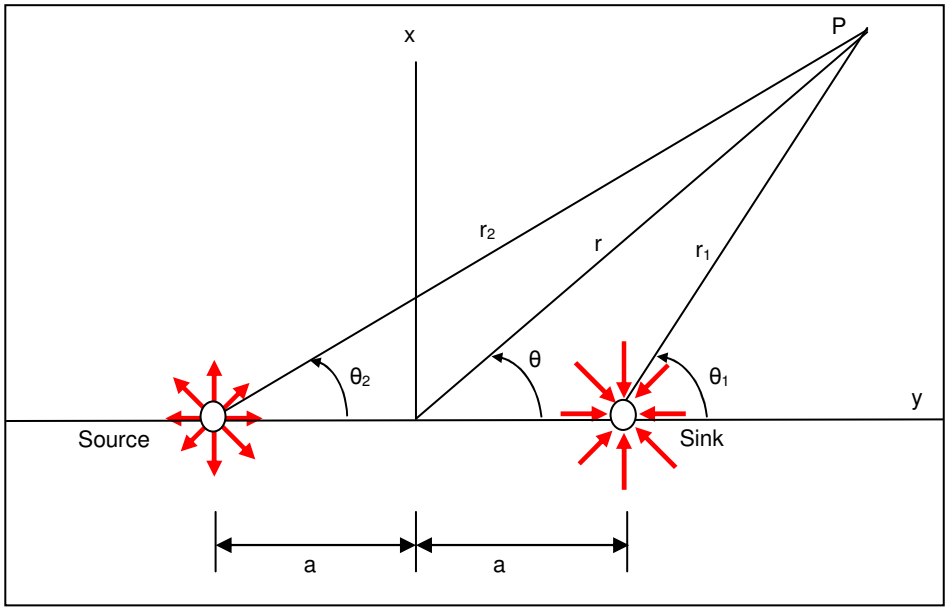

Figure 2.3. Schematic illustration of doublet.

$$-\frac{2\pi\psi}{m} = (\theta_1 - \theta_2) \tag{2.32}$$

If tangent of the above equation is taken:

$$\tan\left(-\frac{2\pi\psi}{m}\right) = \tan(\theta_1 - \theta_2) = \frac{\tan\theta_1 - \tan\theta_2}{1 + \tan\theta_1 \tan\theta_2} \tag{2.33}$$

From Figure 2.1.3; tanθ_1 and tanθ_2:

$$\tan\theta_1 = \frac{r\sin\theta}{r\cos\theta - a} \qquad \tan\theta_2 = \frac{r\sin\theta}{r\cos\theta + a} \tag{2.34}$$

Substitution of Equation 2.34 in equation 2.33 will result:

$$\tan\left(-\frac{2\pi\psi}{m}\right)=\frac{2ar\sin\theta}{r^2-a^2} \tag{2.35}$$

Since the tangent of an angel approaches the value of the angle for small angles (Munson et al. 2002):

$$\begin{aligned}-\frac{2\pi\psi}{m}&=\frac{2ar\sin\theta}{r^2-a^2}\\ \psi&=-\frac{mar\sin\theta}{\pi(r^2-a^2)}\end{aligned} \tag{2.36}$$

The doublet is formed by letting the source and sink approach one another ($a\rightarrow 0$) while the increasing the strength m ($m\rightarrow\infty$) so that the product ma/π remains constant (Munson et al. 2002). In this case, since $r/(r^2-a^2)\rightarrow 1/r$, Equation2.1.36 reduces to:

$$K=\frac{ma}{\pi} \qquad\qquad \psi=-\frac{K\sin\theta}{r} \tag{2.37}$$

Similarly, velocity potential of doublet could be explained:

$$\psi=-\frac{K\cos\theta}{r} \tag{2.38}$$

2.1.11. Flow around a Cylinder and Sphere

When the distance between source and sink in doublet approaches the zero, the shape of the doublet will be blunter. If a doublet is combined with a uniform flow in positive x direction, flow around a circular cylinder can be represented. Stream function for flow around cylinder:

$$\begin{aligned}\psi&=\psi_{UniformFlow}+\psi_{Doublet}\\ \psi&=U.r.\sin\theta-\frac{K\sin\theta}{r}\\ \psi&=r\sin\theta\left(U-\frac{K}{r^2}\right)\end{aligned} \tag{2.39}$$

Stream function will be zero when r equals to the radius of the cylinder (a).

$$\Psi=0 \text{ @ } r=a \qquad\qquad U-\frac{K}{r^2}=0 \tag{2.40}$$

Then the stream function around a cylinder with radius *a*:

$$\psi = Ur\left(1-\frac{a^2}{r^2}\right)\sin\theta \quad (^{\bullet}) \tag{2.41}$$

The velocity potential for flow around cylinder:

$$\phi = U.r.\cos\theta + K\frac{\cos\theta}{r}$$

$$\phi = r\cos\theta(U+\frac{K}{r^2}) \tag{2.42}$$

$$\phi = Ur\left(1+\frac{a^2}{r^2}\right)\cos\theta \tag{2.43}$$

Two-dimensional flow around a sphere will be similar to the flow around a cylinder. When Eq. 2.41 and Eq. 2.43 are used, the potential flow streamlines could be drawn for a sphere. Through a stream line around a cylinder or sphere, the stream function will be constant. It could be done by help of mathematical software. In this study, streamlines were drawn by Matlab R12.

2.1.12. Potential Flow Streamlines by Simulation

If a solid object is subjected to a uniform flow there will be streamlines around it. Meaning of streamlines is that a flow regime has constant stream function value. If the flow regime around the solid object is painted according the stream function value, each different stream function value will have different color, and then a picture showing the streamlines will be made. The flow regime around a cylinder or sphere must be investigated in cylindrical coordinates. Around a sphere stream functions values will be changed by changing *r* and θ. Each equal stream function values will form the streamlines. Drawing the streamlines by a computer requires solving Eq. 2.41. The Algorithm is given in Figure 2.4 and the whole computer code is given in APPENDIX A.

• Program line (11) in APPENDIX A

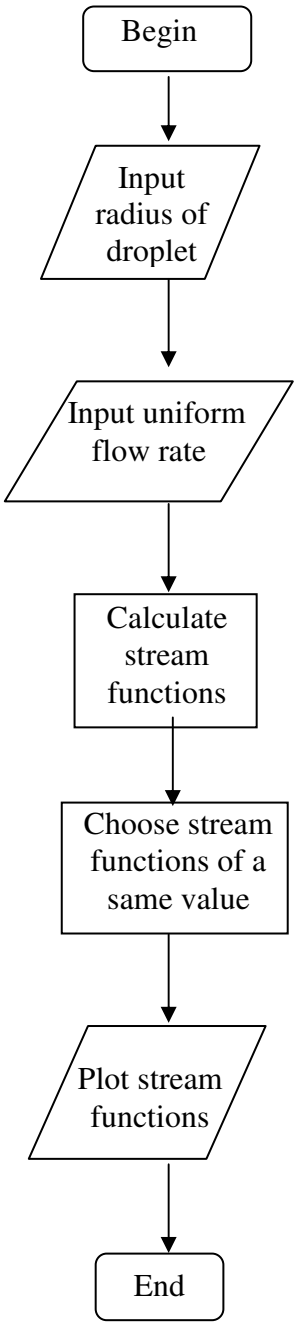

Figure 2.4. Algorithm of drawing potential flow streamlines around a sphere

The uniform flow rate and the radius of the sphere are only variables that affect the stream function as it is seen easily in the Figure 2.5 and 2.6. If these variables are changed, then the streamlines will draw different pictures. As it is seen in the figures, there are no turbulence, eddies and vorticity in the flow field instated of increasing flow rate. This is the result of potential flow theory. Irrotational flow assumption makes the flow field is irrotational. Boundary layer separation is ignored and particle pathways can

be controlled easily by assuming potential flow theory. Streamlines becomes closer to the object and each other with increasing uniform flow rate. Collection efficiency of a particle by a droplet is expected to increase due to increasing uniform flow rate. The streamlines are like uniform flow when radius of sphere is small. If the radius of the droplets is increased, then the shape of the streamlines will be curly. Hence the collection probability of particles can be increased by inertia impaction that a kind of collection mechanism is explained in modeling section. Potential flow theory is important to decide the particle pathways due to uniform flow and remove the complexity form boundary layer separation. A discussion could be made between flow rate and radius of the droplets in order to increase the particle collection efficiency. This discussions and result are used in the modeling and discussions part of the study.

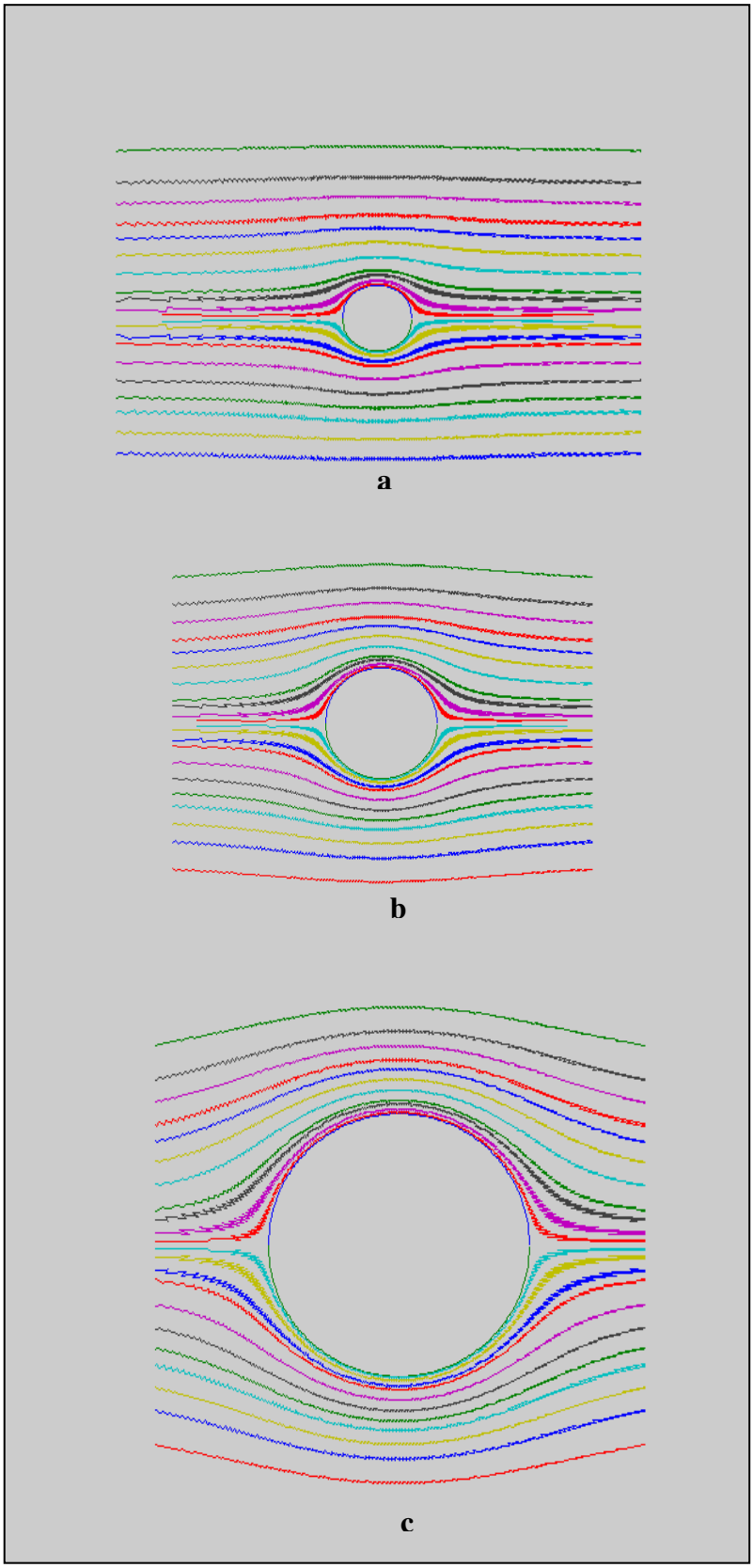

Figure 2.5. Streamlines around a cylinder, (a) r=2m, U=10m/s, (b) r=4m, U=10m/s, (c)r=8m, U=10m/s

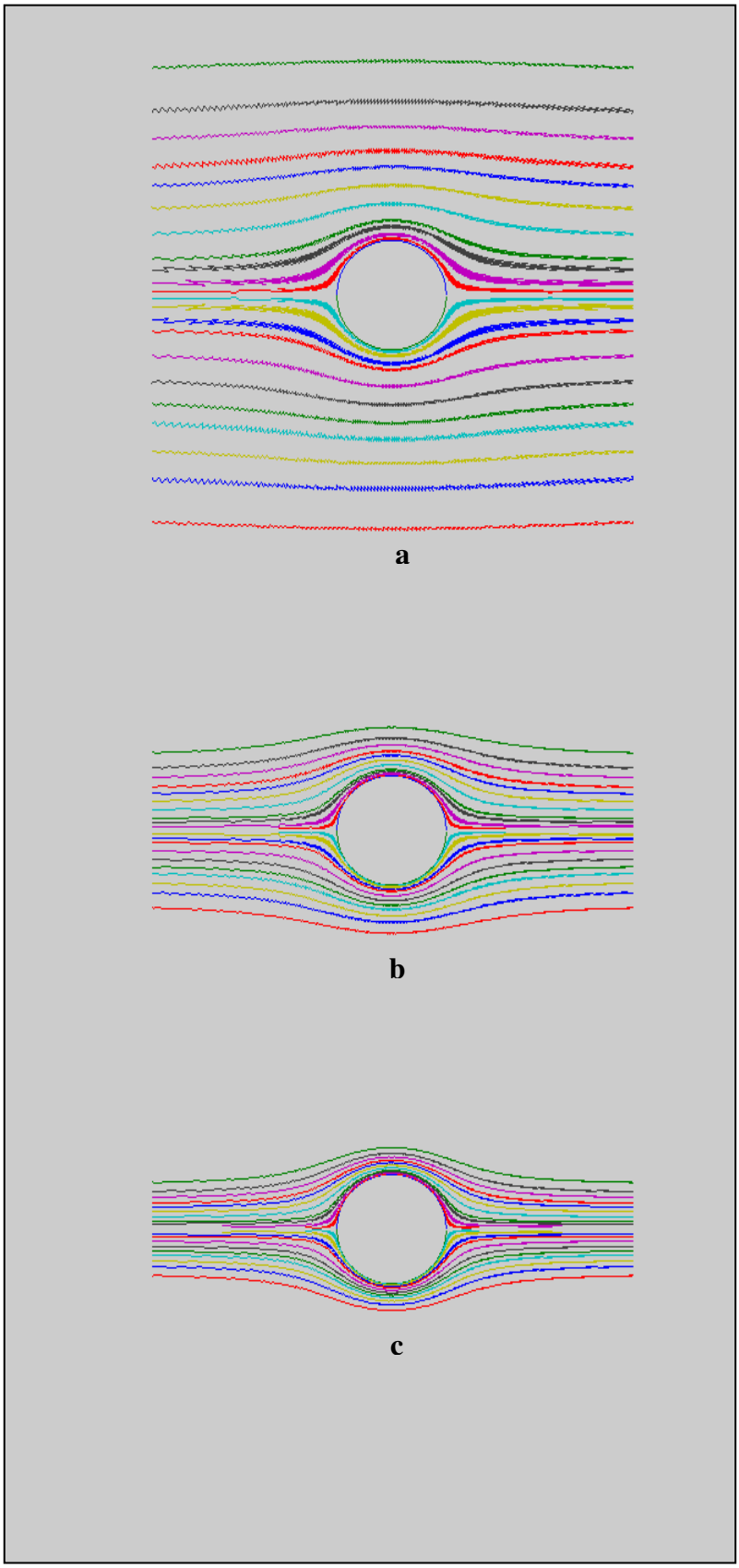

Figure 2.6. Streamlines around a cylinder, (a) r=5m, U=5m/s, (b) r=5m, U=15m/s, (c) r=5m, U=25m/s

2.2. Drag Force

When an object is submersed and moves into fluid a drag will be experienced by the object. This force is called drag force. Pathways of particles and droplets are strongly influenced by this force. Drag force is a function of the particle shape, fluid velocity and friction. The general expression of drag force is given by (Munson et al. 2002):

$$F_D = \frac{1}{2} C_D \rho U^2 A \tag{2.44}$$

Where ρ is the fluid viscosity, U is the uniform flow rate and A is the cross sectional area of the body. The other parameter, C_D, is the drag coefficient. Drag coefficient is a very complex parameter that changes with the shape of the object. It has different values with different fluids, and with different flow rates. Scientists have found that drag coefficient is a strong function of Reynolds number. For small Reynolds numbers (Re<0.5), drag coefficient is expressed as:

$$C_D = \frac{24}{\mathrm{Re}} \tag{2.45}$$

However, there is a complex relationship between drag force and Reynolds number when it is greater than 0.5. This complexity was tried to be solved and there were several approaches, (Concha and Almedra 1979a), (Concha and Almedra 1979b), (Concha and Barrientos 1982), (Concha and Barrientos 1986), (Concha and Christiansen 1986). Concha's approach is one of the best explanations for drag coefficient for systems that are formed suspensions of non-spherical particles. In this study, the particles are suspended in the air and they are non-spherical. Drag coefficient according to Concha is:

$$C_D \cong 0.28\left(1 + \frac{9.06}{\mathrm{Re}^{1/2}}\right)^2 \tag{2.46}$$

Beside of the Reynolds number dependency of the drag coefficient, there is also shape dependency. Figure 2.6 explains the shape dependency of the drag coefficient (Munson et al. 2002). However, Drag coefficients of small objects are not influenced by Reynolds number. Cunningham correction factor is used instead of drag coefficient for so small objects.

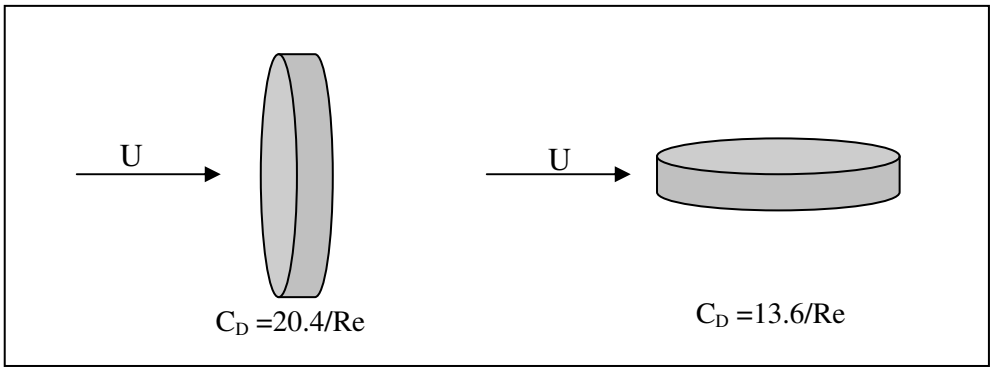

Figure 2.7. Drag coefficients for different cross sectional areas

2.2.1 Cunningham Correction Factor

Particle size will be comparable with the gas mean free path for very small particles. Slip occurs at this stage and drag is needed to be modified. Cunningham obtained the needed correction to the drag force (WEB_1 2005).

$$F_D = \frac{3\pi\mu U d}{C_c} \tag{2.47}$$

Where, C_c is the Cunningham correction factor replaced with the drag coefficient. It is described as:

$$C_c = 1 + \frac{2\lambda}{d}\left[1.257 + 0.4e^{-\frac{1.1d}{2\lambda}}\right] \tag{2.48}$$

Where, λ is molecular mean free path in the gas. It is described as:

$$\lambda = \frac{23.1T}{P}\,(\mu\,\mathrm{m}) \tag{2.49}$$

In this study, the particles and the droplets are so small; therefore Equation 2.2.4 will be used with Cunningham correction factor in order to express drag force.

2.3. Van der Waals Forces

Bodies have been interacting since the beginning of the universe. These bodies are not macroscopic; but also microscopic; such as planets, atoms, stars, rocks, metals, electrons etc. Liquid droplets and dust particles interact with each other, so that

collection occurs. Interaction energy and force due to this energy have been studied. One of the most important interactions is Van der Waals interactions, which will be presented in this section.

Van der Waals interaction is an internal interaction between particulate matters since the distance between the bodies is comparable with their sizes when this kind of interaction is dominant on the bodies. Van der Waals interaction does not occur between only macroscopic bodies, but also it occurs in microscopic bodies. First; it was studied for atoms and molecules. Then the theory was applied to macroscopic bodies. Finally; simple equations were obtained to express the Van der Waals forces. In this section, microscopic and macroscopic forms of Van der Waals interaction are going to be reviewed and an equation will be obtained in order to use for model in this study.

2.3.1. Van der Waals Interaction between Microscopic Bodies

If molecules and atoms have permanent dipole moments, attraction forces occur between them. An attraction force will be exerted by one molecule on the other molecule since both of them have permanent dipole moments. Keesom studied this interaction. This kind of relationship between atoms and molecules is known as Keesom equation (Polat H. and Polat M. 2000).

$$\phi_K = -\frac{2}{3}\frac{\mu_1^2\mu_2^2}{kT(4\Pi\varepsilon_o)^2 x^6} \tag{2.50}$$

For identical molecules, Keesom equation turns out to be;

$$\phi_K = -\frac{2}{3}\frac{\mu^4}{kT(4\Pi\varepsilon_o)^2 x^6} \tag{2.51}$$

Sometimes one molecule can have permanent dipole moment while the other does not have. However; permanent dipole moment of one molecule will induce a dipole moment in a second molecule irrespective of whether the second molecule has a permanent dipole moment (Polat H. and Polat M. 2000). The interaction energy was calculated for two molecules; one has permanent dipole moment and the other has induced dipole moment by Debye.

$$\phi_D = -\frac{(\alpha_{0,2}\mu_1^2 + \alpha_{0,1}\mu_2^2)}{(4\Pi\varepsilon_o)^2 x^6} \tag{2.52}$$

For two identical molecules, Debye equation becomes:

$$\phi_D = -\frac{2\alpha_0\mu^2}{(4\Pi\varepsilon_o)^2 x^6} \tag{2.53}$$

There will be an attractive force when both of the molecules have no permanent dipole moment. Electrons turn around the nucleus. Electron density might concentrate on one side of the atom at some moment. Therefore, instantaneous dipole moments will be developed. This instantaneous dipole moment will induce a dipole moment on the other molecule. There will be an attraction between the molecule with instantaneous dipole moment and the other molecule with induced dipole moment. London expressed this attraction force as (Polat H. and Polat M. 2000):

$$\phi_L = -\frac{3}{2}h\left(\frac{V_{0,1}V_{0,2}}{V_{0,1}+V_{0,2}}\right)\frac{\alpha_{0,2}\alpha_{0,1}}{(4\Pi\varepsilon_o)^2 x^6} \tag{2.54}$$

For two identical molecules:

$$\phi_L = -\frac{3}{4}\frac{hV_0{\alpha_0}^2}{(4\Pi\varepsilon_o)^2 x^6} \tag{2.55}$$

Two important points must be discussed at this stage. There is a common term in all the three interactions. This is the 6th inverse power of the separation distance of the molecules. Although Keesom and Debye need at least one permanent dipole moment, London does not. Keesom, Debye and London interactions are illustrated in Figure 2.8.

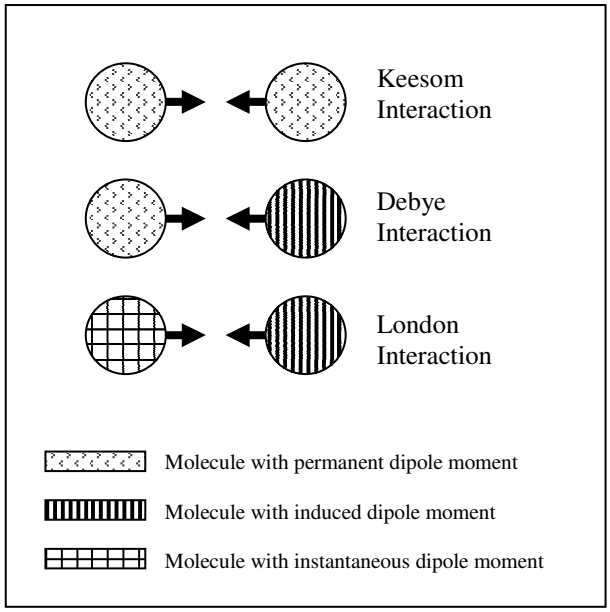

Figure 2.8. Schematic illustration of Keesom, Debye and London attractive interactions.

The sum of these three interaction energies is called Van der Waals interaction [12].

$$\phi_{VdW} = \phi_K + \phi_D + \phi_L \tag{2.56}$$

$$\phi_{VdW} = -\left[\frac{\frac{2\mu^4}{3kT} + 2\alpha_0\mu^2 + \frac{3hV_0\alpha_0^2}{4}}{(4\Pi\varepsilon_0)^2}\right]x^{-6} \tag{2.57}$$

If all the terms inside the parenthesis are gathered in a constant.

$$\phi_{VdW} = -\beta_{11}x^{-6} \tag{2.58}$$

Finally; derivation of Eq. 2.58 with respect to *x* will give the Van der Waals force.

$$F_{VdW} = \frac{d\phi_{VdW}}{dx} = 6\beta_{11}x^{-7} \tag{2.59}$$

For all molecules or atoms Van der Waals forces can be calculated by utilizing the Eq. 2.59. As it is seen in Eq. 2.56, Van der Waals force is a function of Keesom, Debye and London equations. While London interaction is dominant for some matters; Keesom and Debye is dominant for other matters. For example; % 85 of Van der Waals force for polar molecules is due to Keesom and Debye while all the force for polar molecules is due to London (Polat H. and Polat M. 2000).

2.3.2. Van der Waals Interaction between Macroscopic Bodies

Van der Waals interactions between microscopic bodies such as atoms and molecules were discussed, above. However; interaction of macroscopic bodies was an unknown subject for scientists. Hamaker developed a theory that explains the Van der Waals interactions between macroscopic bodies. This theory is called microscopic approach since it depends on the microscopic equations. Details of the Hamaker theory for macroscopic bodies are summarized below.

Let us take two infinitely long plates having thickness of δ, and separated from each other with distance *H*. Let us also assume second plate has a ring in it. Thickness of the ring that is *dr*, inner radius is r and width of it is *dh*. Schematic illustration of the ring is shown in Figure 2.9. The number of atoms in this ring will be:

$$N_2 = 2.\pi.r\left(\frac{\rho_2.N_A}{M_2}\right)dr.dh \tag{2.60}$$

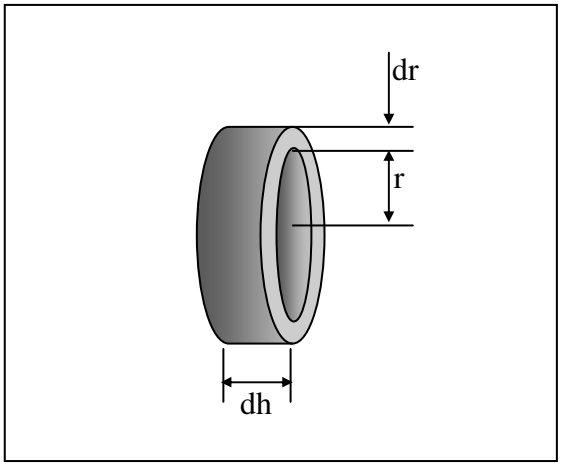

Figure 2.9. Schematic illustration of the ring assumed in microscopic approach

where, $\rho_2 N_A / M_2$ is the number of atoms per unit volume for the second plate. The slabs and their geometry are illustrated in Figure2.10.

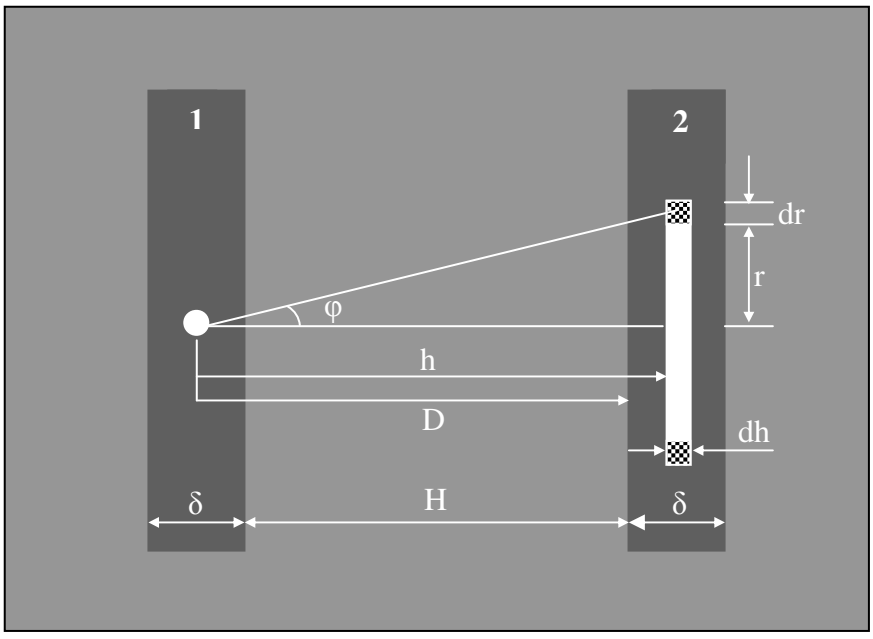

Figure 2.10. Schematic illustration of the geometry of infinite slabs used for calculation of Van der Waals Forces (Polat H. and Polat M. 2000).

Only one atom is chosen in slab 1 while a ring is chosen in slab 2 as it is seen in Figure2.10. The Van der Waals interaction between this atom and the ring can be formulated due to the Eq. 2.59.

$$F_{12}^{'} = 12.\pi.r\left(\frac{\rho_2 N_A}{M_2}\right) Cos\varphi.\beta_{12} x^{-7} dh.dr \tag{2.61}$$

From the geometry in the Figure 2.10., the "*x*" and "*cosφ*" are defined as $x = \sqrt{r^2 + h^2}$ and $Cos\varphi = h/\sqrt{r^2 + h^2}$. The Eq. 2.61 expresses the attractive interaction of an atom and a ring. Integration of Eq. 2.61 with respect to *h* and *r* will give the attractive interaction between an atom and the second plate.

$$F_{12}^{'} = 12.\pi.\left(\frac{\rho_2 N_A}{M_2}\right)\beta_{12}\int_{r=0}^{\infty} r\left[\int_{h=D}^{D+\delta}\frac{h}{(r^2+h^2)^4}dh\right]dr \tag{2.62}$$

Integrating the Eq. 2.62 with respect to *h* gives:

$$F_{12}^{'} = -2.\pi.\left(\frac{\rho_2 N_A}{M_2}\right)\beta_{12}\int_{r=0}^{\infty}\left[\frac{1}{r^2+(D+\delta)^2} - \frac{1}{r^2+D^2}\right]dr \tag{2.63}$$

Integrating the Eq. 2.63 with respect to r gives:

$$F_{12}^{'} = \frac{\pi}{2}.\left(\frac{\rho_2 N_A}{M_2}\right)\beta_{12}\left[\frac{1}{D^4} - \frac{1}{(D+\delta)^4}\right] \tag{2.64}$$

Above equation has not been adequate to express the attractive interaction between macroscopic bodies yet. Eq. 264 gives the relationship for an atom and all atoms in slab 2. The interaction force for all atoms in slab 1 and 2 can be explained in the equations below:

$$F_{VdW} = \int_{H}^{H+\delta} F_{12}^{'} dV_1 \tag{2.65}$$

$$F_{VdW} = \frac{\pi}{2}.\left(\frac{\rho_1 N_A}{M_1}\right)\left(\frac{\rho_2 N_A}{M_2}\right)\beta_{12}\int_{H}^{H+\delta}\left[\frac{1}{D^4} - \frac{1}{(D+\delta)^4}\right]dD \tag{2.66}$$

The solution of above equation is the force of interaction per unit area of the slabs between two infinitely wide slabs separated by distance H [12];

$$F_{VdW} = \frac{\pi}{6}.\left(\frac{\rho_1 N_A}{M_1}\right)\left(\frac{\rho_2 N_A}{M_2}\right)\beta_{12}\left[\frac{1}{H^3} + \frac{1}{(H+2\delta)^3} - \frac{2}{(H+\delta)^3}\right] \tag{2.67}$$

Above equation can be considered as Van der Waals interaction between macroscopic bodies when the thickness of slab approaches infinity ($\delta \rightarrow \infty$).

$$F_{VdW} = \frac{A}{6.\pi.H^3} \tag{2.68}$$

where, *A* is called as Hamaker Constant and it has the form.

$$A_{12} = \pi^2 \left(\frac{\rho_1 N_A}{M_1} \right) \left(\frac{\rho_2 N_A}{M_2} \right) \beta_{12} \tag{2.69}$$

2.3.3 Retardation Effect

Van der Waals attraction interaction is due to the dipole moments of the molecules as discussed above. According to London interaction, both of the atoms have no permanent dipole moment. Attractive interaction occurs because electron density around the nucleus focused on one side of the atom at some moment. This causes an instantaneous dipole moment. Time is an important parameter for London interaction. At another time the electron density can change and the electron orientation caused by instantaneous dipole moment can disappear. The time needed for the electromagnetic field of an instantaneous dipole to reach a neighboring atom and return must be shorter than the time it takes for an electron to complete its orbit around the atom. However; if two atoms are widely separated from each other, the time needed for the electromagnetic field of an instantaneous dipole to reach a neighboring atom and return may be comparable with the fluctuation period itself. If separation distance is smaller Eq. 2.68 is valid, however, if the separation distance is greater than 10 nm a correction must be made to the equation (Polat H. and Polat M. 2000). In literature many equations are known as retarded and non-retarded Van der Waals interactions. In this study, the proper equation will be chosen according to our system and its separation distance.

2.3.4. Macroscopic Approach

Hamaker makes a good approach in order to express the attractive interaction between macroscopic bodies. This approach is investigated in previous section. Although, it is a good theory, there are some discussible points.

Integration was done to achieve the macroscopic relation from the microscopic form. Integrating means cumulative of the microscopic interactions. However, to consider the pair wise additivity of molecular interactions is not valid for all systems. If the system dealing with is rarefied the approach will be true. Hamaker's theory does not distinguish between the surface and the bulk molecules. The interaction of the

molecules that are inside of the macroscopic body may be screened by the molecules at the surface.

Interaction energy can be influenced by the separation medium. This effect is not considered in Hamaker's theory. However, medium has strong influence on the system, even the sign of the interaction energy may change.

Retardation effect was also neglected in the Hamaker's theory. These problems were solved by Liftshitz and Pitaevski . There are also molecular parameters that are unavailable to measure in Hamaker's theory. However, measurable bulk parameters are used and three discussible points of Hamaker's theory discussed above are solved in the new theory. According to Liftshitz and Pitaevski, Van der Waals force between two macroscopic body separated by a medium in terms of dielectric constant is given as:

$$F_{132} = \frac{h}{8.\pi^2.H^3}\int_0^\infty \sum_{n=1}^{\infty} \left[\frac{1}{n^3}\left(\frac{\varepsilon_1(i\xi)-\varepsilon_3(i\xi)}{\varepsilon_1(i\xi)+\varepsilon_3(i\xi)}\right)\left(\frac{\varepsilon_2(i\xi)-\varepsilon_3(i\xi)}{\varepsilon_2(i\xi)+\varepsilon_3(i\xi)}\right)\right]^n d\xi \tag{2.70}$$

If all the integral above equation is defined as ω, the Eq. 2.70 will be:

$$F_{132} = \frac{h\omega_{132}}{8.\pi^2.H^3} \tag{2.71}$$

hω is known as Liftshitz constant. If we equate the Eq. 2.68 and 2.71, a true relationship will be found between Hamaker's constant and Liftshitz constant.

$$A = \frac{3}{4\pi} h\omega \tag{2.72}$$

2.3.5. Hamaker Constants

Hamaker constants of species are important parameters for systems in order to predict the Van der Waals interaction in the system. There is also a true relationship between Liftshitz and Hamaker constants so that the Liftshitz constant can be calculated from the Hamaker constant. Scientists have been studied to find the Hamaker constant's of the species. There are three main ways. The first way is the microscopic procedure. Hamaker constants were calculated from microscopic parameters in this method. The second method deals with Liftshitz theory. In this method called as macroscopic procedure the macroscopic bulk parameters are used by. In the third method experiments are used to determine.

Separation medium has an important effect on Van der Waals interaction. This effect must be included in the equation. Liftshitz considered that in his theory. Hamaker constant of separation medium must be added to overall Hamaker constant of the system. There are two bodies 1 and 2 separated with a separation medium 3 then the effective Hamaker constant will be A_{132}. This relation can be formulated as pseudo-chemical reaction. The schematic illustration of thermodynamics way of pseudo chemical reaction is shown in Figure 2.3.4.

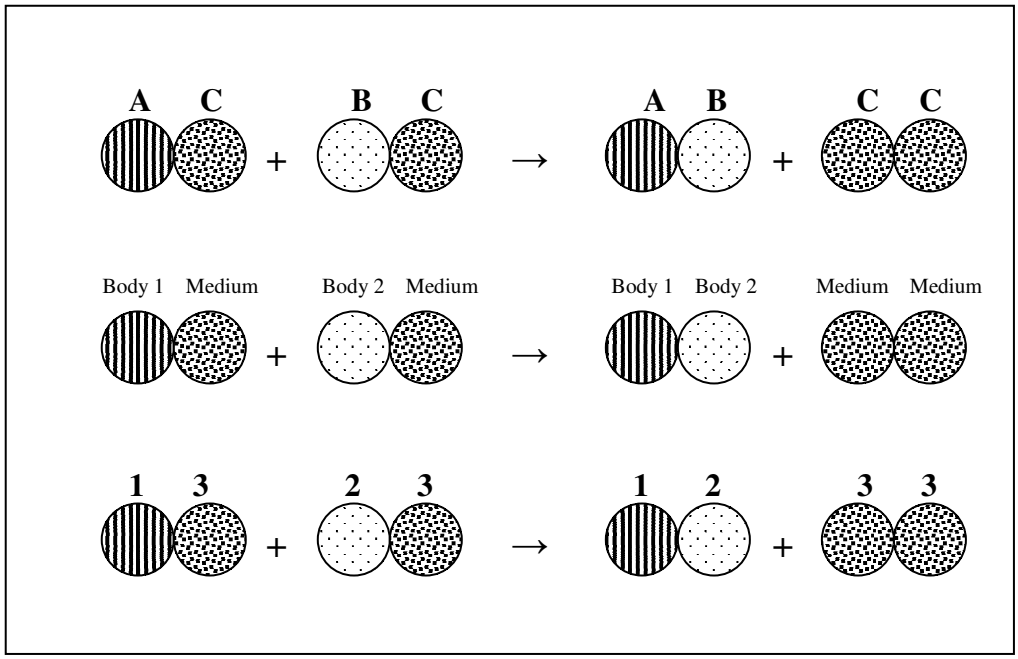

Figure 2.11. Schematic illustration of the pseudo-chemical reaction between bodies and medium.

Thermodynamically way of pseudo-chemical reaction in Figure 2.3.4 is used to calculate the potential energy change of the system. If the separation distance is kept as a constant the Hamaker constant of the system will be true proportional to the potential energy change of the system.

$$A_{132} = A_{12} + A_{33} - A_{13} - A_{23} \tag{2.73}$$

The interaction between two particles i and j can be given by the geometric mean of the interaction between i-i and j-j pairs to a good approximation as:

$$A_{ij} = \sqrt{A_{ii} A_{jj}} \tag{2.74}$$

then;

$$A_{132} = \left(\sqrt{A_{22}} - \sqrt{A_{33}}\right)\left(\sqrt{A_{11}} - \sqrt{A_{33}}\right) \tag{2.75}$$

Hamaker constants values of species were calculated in the literature by using different methods. These are available in the literature. Effective Hamaker constant of a system can be calculated using Eq. 2.75. Van der Waals interaction is effected by Hamaker constant value even is sign can change. Effect of this constant can be summarized as:

1. Van der Waals interaction always decreases between particles placed in a medium. In Hamaker's theory does not account for this decrease while in Liftshitz theory this effect is included.

2. If two macroscopic bodies are the same, the interaction will change strongly according to the medium. If medium's Hamaker constant is identical with bodies also, the interaction will be zero. Otherwise the interaction energy will always be positive.

3. If the bodies are not identical, there will be three different situations. If the Hamaker constant of one of the particles is equal to the medium, the interaction between particles will be zero. If the medium's Hamaker constant is between the Hamaker constants of the particles, then the Van der Waals interaction will be negative. It is only the situation that Van der Waals interaction is repulsive not attractive. Otherwise the interaction will be positive.

As a conclusion Hamaker constant is a function of Hamaker constant and separation distance. In this study, spherical particles are considered. The Van der Waals equations for two different spherical particles are given below. Application of this equation is illustrated in Figure 2.11.

$$F_{VdW} = \frac{A.R_1.R_2}{6.H^2.(R_1 + R_2)} \tag{2.76}$$

As it is seen in the Figure 2.11, the Van der Waals interaction is a strong force when the bodies are closed to each other, otherwise the interaction will be weak. Thus study deals with liquid water droplet and a quartz particle in spherical form. The

separation medium is chosen as air. Separation distance is smaller than the diameters of the particles.

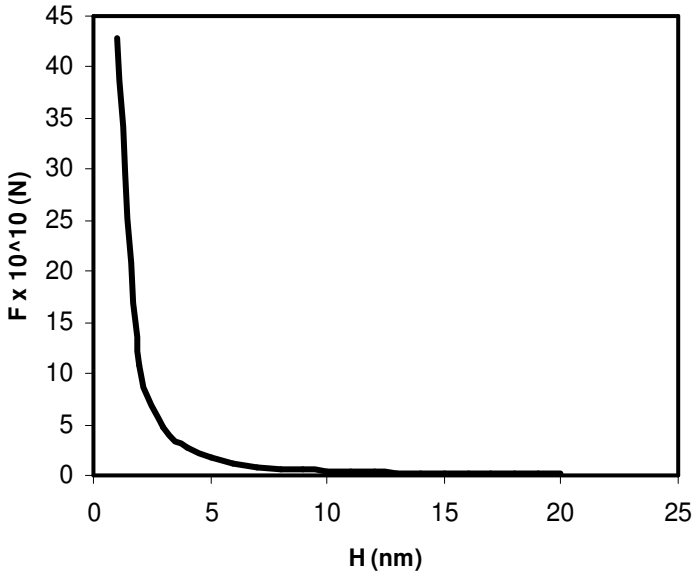

Figure 2.11. Van der Waals force versus separation distance for quartz-water and air system; radius of quartz particle is 1 μm, radius of water droplet is 6 μm, and Hamaker constant $A=5x10^{-20}$ J.

2.4. Electrostatic Interactions

Electrostatic interactions are the most effective interactions that occur at the electrical double layer of the particles and droplets due to their electrostatic potential. Electrical double layer and Gouy-Chapman model will be explained firstly**.**

2.4.1. Electrical Double Layer

When two different phases are brought into contact, there will be electrical double layer. Change of the any property "p" has been an important subject. The p will be p_α in α phase while this property has p_β in β phase. These values do not equal to each other. If there is no double layer, there will be a sudden increase or sudden decrease for the value of p. The schematic illustration of the electrical double layer is shown in Figure 2.12.

The value of property p is changing regularly in double layer. The areas in Figure 2.4.1 have important role in characteristics of double layer. The upper area is called as surface excess while the below one is called as surface deficiency. The surface excess and the surface deficiency should be equal to each other. The vertical line between them is called Gibbs dividing surface when these areas equal to each other.

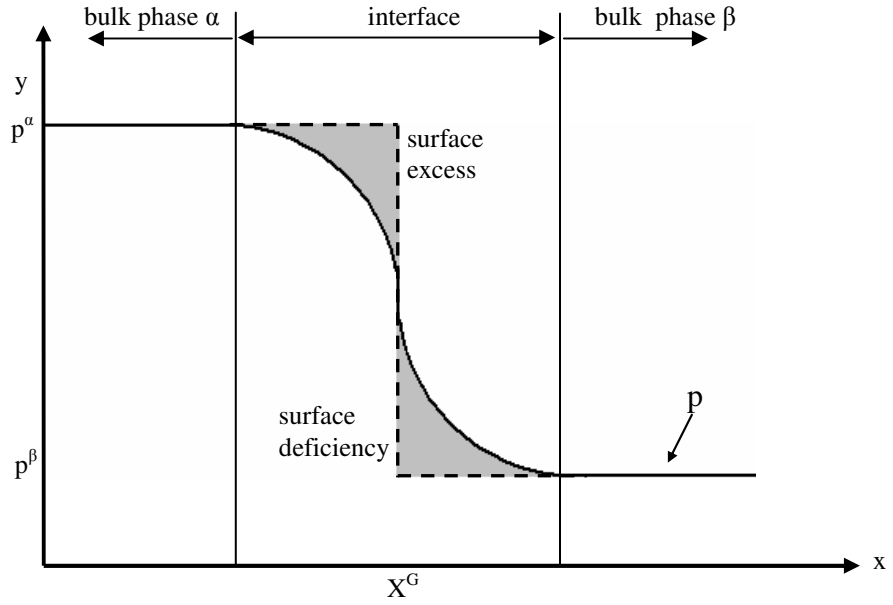

Figure 2.12. Variation of a property p at an interface between phases α and β.

There are several theories that express this phenomena in electrical double layer. The most important ones are The Helmhlotz Model, The Gouy-Chapman Model, and Stern Model (Polat 1999). In this study, the Gouy-Chapman model will be investigated in order to express the electrostatic interaction between macroscopic bodies because it explains the electrical double layer better and is easy to apply.

2.4.2. Gouy-Chapman Model

Gouy-Chapman model explains the electrostatic potential of a particle in terms of distance from the surface of the particle through the solution. Electrostatic potential of a molecule or atom determines the electrostatic behavior and interaction of it. The main assumption of Gouy-Chapman model is that there exist several plates with thickness of *dx* and these plates are in thermal equilibrium with each other. The

alignment of them is from the solution through the solution. Each plate has ions and the bulk concentration of ions can be determined by Boltzman Factor.

$$n_i(x) = n_{i,0} \exp\left(-\frac{z_i.e_0.\psi(x)}{k.T}\right) \tag{2.77}$$

Charge density per unit volume at a distance x from the surface is given by (Polat 1999):

$$\rho(x) = \sum_i z_i.e_0.n_i(x) \tag{2.78}$$

If Eq. 2.77 and Eq. 2.78 are combined the charge density will be:

$$\rho(x) = \sum_i z_i.e_0.n_{i,0} e^{-\frac{z_i.e.\psi(x)}{kT}} \tag{2.79}$$

Poisson equation gives the relationship between charge density and electrostatic potential:

$$\rho(x) = -\varepsilon.\varepsilon_0 \frac{d^2\psi(x)}{dx^2} \tag{2.80}$$

If equation 2.4.3 is dumped into Eq. 2.80:

$$\frac{d^2\psi}{dx^2} = -\frac{1}{\varepsilon.\varepsilon_0} \sum_i z_i.e_0.n_{i,0}.e^{-\frac{z_i e_0 \psi}{kT}} \tag{2.81}$$

Some simplifications could be done in Eq. 2.81. For example, $e_0.n_{i,0}$ term can be replaced with $F.C_{i,0}$ and also e_0/k term can be rewritten as F/R. Therefore, Eq. 2.81 changes to:

$$\frac{d^2\psi}{dx^2} = -\frac{F}{\varepsilon.\varepsilon_0} \sum_i z_i.C_{i,0}.e^{-\frac{z_i F \psi(x)}{RT}} \tag{2.82}$$

Eq. 2.82 is known as Poisson Boltzman equation. The exponential term in Poisson-Boltzman equation can be expanded in series. Furthermore; the first term of the series will be zero since solution is electro neutral.

$$\frac{d^2\psi}{dx^2} = -\frac{F}{\varepsilon.\varepsilon_0}\left[\sum_i z_i.C_{i,0} - \sum_i z_i.C_{i,0}.\frac{z_i F \psi(x)}{RT}\right] \tag{2.83}$$

$$\frac{d^2\psi}{dx^2} = \left(\frac{F^2}{\varepsilon.\varepsilon_0.RT} \sum_i z_i^2 C_{i,0}\right)\psi \tag{2.84}$$

If all the parameters in parenthesis are dumped into a parameter κ^2, the Eq. 2.84 will be:

$$\kappa = \sqrt{\frac{F^2}{\varepsilon.\varepsilon_0.RT}} \cdot \sqrt{\sum_i z_i{}^2 C_{i,0}} = \sqrt{\frac{F^2}{\varepsilon.\varepsilon_0.RT}} \sqrt{I} \tag{2.85}$$

$$\frac{d^2\psi}{dx^2} = \kappa^2 \psi \tag{2.86}$$

Eq. 2.86 is known as Debye-Hückel equation and it is an effective relationship for expression of the electrostatic interaction between macroscopic bodies.

2.4.3. Electrostatic Interactions

When a particle is placed in a fluid medium, there exists a double layer on the particle that has electrostatic potential Ψ_0 and charge σ^s and; there exists a diffuse layer on the liquid surface that has sign and potential to neutralize the particle. This system is important on electrostatic interaction of particles. There are several modeling studies in order to understand and calculate the double layer.

The electrostatic interaction between two spherical objects is hard to determine. Therefore, system must be simplified. Firstly, two plates having double layer could be considered. However; the electrostatic potential and charge of the electrical double layer is not constant in real system. It is a function of time. The main assumption must be an important assumption that plates have constant surface potential and constant surface charge. At this point, there are several studies in order to explain this system. The most important theory is due to Gouy-Chapman model as it is mentioned previously. The electrostatic potential change with respect to x is given by Eq. 2.86 according to the Gouy–Chapman model. Assumptions that there are two flat plates with constant electrostatic potentials $\Psi_{0,1}$ and $\Psi_{0,2}$ must be made in order to integrate the equation. Boundary conditions will be:

$\psi = \psi_{0,1}$ @ $x = 0$

$\psi = \psi_{0,2}$ @ $x = H$

The solution of Eq. 2.86 according to above boundary conditions will be:

$$\psi_{12} = \psi_{0,1} \cosh \kappa x + \left(\frac{\psi_{0,2} - \psi_{0,1} \cosh \kappa H}{\sinh \kappa H} \right) \sinh \kappa x \tag{2.87}$$

Potential energy of this electrostatic interaction, V'_{el} , is equal to the change in free energy of the double layer system when the plates are brought together from infinity to distance H (Polat H. and Polat M. 2000b), Then;

$$V_{el}^{'} = \Delta G = G_H - G_\infty \tag{2.88}$$

According to Verwey and Overbeek, the free energy of a single double layer with constant electrostatic surface potential:

$$G = -\frac{1}{2}\sigma^s \psi_0 \tag{2.89}$$

The free energy of two interaction double layer will be sum of the free energies of the separate double layers. According to Eq. 2.89:

$$G_H = -\frac{1}{2}(\sigma_1{}^s \psi_{0,1} + \sigma_2{}^s \psi_{0,2}) \tag{2.90}$$

Charge density at a plane surface is given as:

$$\sigma^s = -\varepsilon.\varepsilon_0 \left(\frac{d\psi}{dx}\right)\Big|_{x=0} \tag{2.91}$$

The derivative of Eq. 2.87 is combining with the Eq. 2.91, and then the charge density of each plate will be:

$$\begin{aligned} \sigma_1^s &= -\varepsilon.\varepsilon_0 \kappa \left(\psi_{0,2} \cos ech\,\kappa H - \psi_{0.1} \coth \kappa H\right) \\ \sigma_2^s &= -\varepsilon.\varepsilon_0 \kappa \left(\psi_{0,2} \coth \kappa H - \psi_{0.1} \cos ech\,\kappa H\right) \end{aligned} \tag{2.92}$$

If Eq. 2.92 is combined with Eq. 2.90, then the result will be:

$$G_H = \frac{\varepsilon.\varepsilon_0.\kappa}{2}\left[2.\psi_{0,1}\psi_{0,2} \cos ech\,\kappa H - (\psi_{0,1}^2 + \psi_{0,2}^2)\coth \kappa H\right] \tag{2.93}$$

If the plates are separated from each other, the free energy will be:

$$G_\infty = -\frac{\varepsilon.\varepsilon_0 \kappa}{2}\left(\psi_{0,1}^2 + \psi_{0,2}^2\right) \tag{2.94}$$

Finally potential energy of electrostatic interaction between two plate separated from each other with H will be:

$$V_{el}^{'} = \frac{\varepsilon.\varepsilon_0.\kappa}{2}\left[(\psi_{0,1}^2 + \psi_{0,2}^2)(1 - \coth \kappa H) + 2\psi_{0,1}\psi_{0,2} \cos ech\,\kappa H\right] \tag{2.95}$$

Above equation gives the relationship of electrostatic potential energy change of two infinitely long and parallel plates per unit area. This energy change is a function of surface potential of the plates and the distance between plates.

However, there are spherical objects in this study. The geometry in equation 2.4.19 must be changed. Hogg used the Derjaguin's approximation in order to change the geometry in Eq. 2.95. In Derjaguin's approximation the thickness of the double layer is assumed to be small compared to the particle size ($\kappa^{-1} << R$). Hence the spherical particles may be assumed to be made up of infinitely thin parallel rings each with its

own double layer stacked on the top of each other (Polat H. and Polat M. 2000a). Each ring will be considered as flat plate with area 2πrdh when h approaches to zero. The differential interaction energy for a ring will be:

$$dV_{el} = 2\pi r V_{el}^{'} dh \tag{2.96}$$

Eq. 2.96 must be integrated in order to calculate the total interaction energy.

$$V_{el} = \int_0^{\infty} 2\pi h V_{el}^{'} dh \tag{2.97}$$

The related geometry for calculation of the electrostatic interaction energy between two spherical particles is illustrated in Figure 2.4.2.

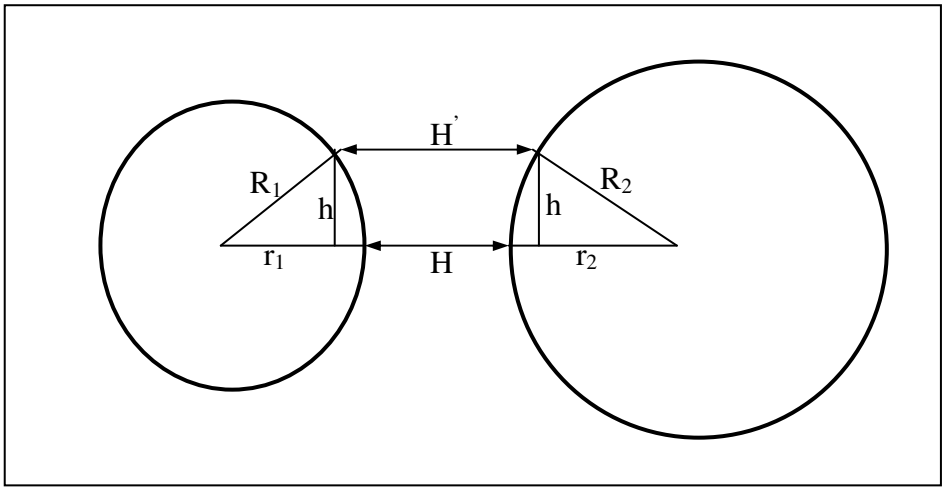

Figure 2.13. Geometry for calculation of the electrostatic interaction energy between two spherical particles.

From Figure 2.13;

$$H^{'} - H = (R_1 - r_1) + (R_2 - r_2) = \left(R_1 - \sqrt{R_1^2 - h^2}\right) + \left(R_2 - \sqrt{R_2^2 - h^2}\right) \tag{2.98}$$

$$H^{'} - H = R_1 + R_2 - \sqrt{R_1^2 - h^2} - \sqrt{R_2^2 - h^2} \tag{2.99}$$

Differentiating with respect to *H* gives:

$$dH = \left(\frac{1}{R_1 \sqrt{1 - h^2 / R_1^{\,2}}} + \frac{1}{R_2 \sqrt{1 - h^2 / R_2^2}} \right) \text{hdh} \tag{2.100}$$

h→0:

$$dH = \left(\frac{1}{R_1} + \frac{1}{R_2} \right) hdh \tag{2.101}$$

$$hdh = \left(\frac{R_1 R_2}{R_1 + R_2} \right) dH \tag{2.102}$$

If Eq. 2.95 and Eq. 2.102 are inserted in Eq. 2.97, the electrostatic potential between two spheres will be:

$$V_{el} = \pi \varepsilon \varepsilon_0 \kappa \left(\frac{R_1 R_2}{R_1 + R_2} \right) \left(\psi_{0,1}^2 + \psi_{0,2}^2 \right) \left[\frac{2\psi_{0,1}\psi_{0,2}}{(\psi_{0,1}^2 + \psi_{0,2}^2)} \ln\left(\frac{1 + e^{-\kappa H}}{1 - e^{-\kappa H}} \right) + \ln\left(1 - e^{-2\kappa H}\right) \right] \tag{2.103}$$

The general solution of interaction between the electrical double layer surrounding two spherical colloidal particles is given by Eq. 2.103. As it is seen in the above equation, the Ψ of the particles is not easy to measure. A simplification is needed to calculate the electrical potential. Electrokinetic potential (ζ) that is easily measured can be used instead of electrostatic potential (Ψ). The justification of this consideration is proved by experimental works of Usui and Yamasaki (1967-1969). Electrostatic interaction has either negative or positive sign.

2.5. Calvert Model

Particle collection efficiencies by liquid droplets generally are examined by experiments. Analytical and numeric models have been developed due to the experiments. One of the most famous one is Calvert Model, which is an analytical method to calculate the collection efficiency. Calvert model are widely used due to its simple analytical expression of collection efficiency. However, there is a calibration constant in order to adjust the equation according to the experimental data. There is a term that called as impaction parameter, K. Eq 2.104 and Eq, 2.105 are the definitions of collection efficiency and impaction parameter for Calvert model (Rudnick et al. 1986). Calvert use a 0.35 calibration constant in collection efficiency given by Eq. 2.105.

$$K = \frac{C_c \rho_p D_p^2 \left| U - u_p \right|}{18 \mu D_d} \tag{2.104}$$

$$\eta = \left(\frac{K}{K + 0.35} \right)^2 \tag{2.105}$$

CHAPTER 3

MODELING

The theories are given in previous section are used in order to construct a model that explain the particle collection mechanisms of liquid droplets. As it is seen on the title of this study, the non-regular shape and agglomeration behaviors of the particles are aimed. Some approaches must be done to explain this non-ideal situation.

The collection mechanisms and the forces acting upon the bodies discussed in the previous section cannot be used in every stage of capturing. The capturing mechanism can be divided into three parts. The first part is about the collision of the particles. Gravitational and drag forces will be effective for collision. The second one is adhesion. Van der Waals interactions are effective at this stage while electrostatic interactions are assumed less affective with respect to Van der Waals at this stage. The last mechanism is engulfment that is dealing with the absorption of particles by liquid droplets (Chander et al. 1991).

Collection probability is a number used to quantify collection mechanisms. This probability is a function of probabilities of three different collection mechanisms. Collection probability can be calculated by the product of collision, adhesion and engulfment probabilities.

$$P_{collection} = P_{collision}.P_{adhesion}.P_{engulfment} \tag{3.1}$$

3.1. Shape

Life is not an ideal event. Nothing is regular. This study is about obtaining a model that explains the interactions of non-spherical and agglomerated particles with liquid droplets were expressed the behavior of non-spherical particles groups. All the equations and previous models are based on the regular geometries. However; there must be a real model since a particle and a droplet not single and they do not necessarily have regular shapes. Having non-spherical shape and being agglomerated are the two main problems developing a proper model. Let us try to solve these problems separately.

There are three different coordinate systems in mathematics. These are rectangular, cylindrical and spherical coordinates. All the models and derivations have been done based on these coordinate systems. To describe non identical geometry in this coordinates is a hard work. There must be a simplification for complex shapes. The term that is equivalent diameter (d_e) will be introduced in order to express a non regular shape's characteristics dimension. Equivalent diameter of a non-regular object will be the same with the diameter of a spherical object that has the same volume with that of the non-regular one (Concha and Barrientos 1986). This approach is illustrated in Figure 3.1.

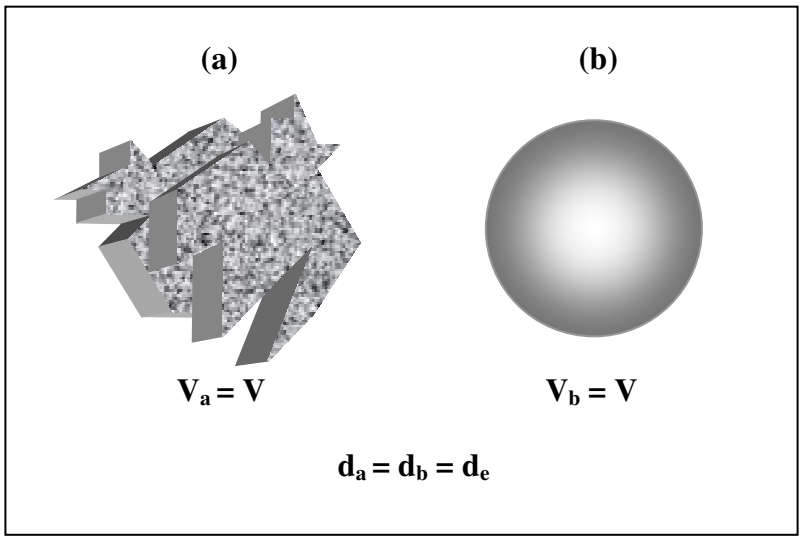

Figure 3.1. Schematic explanation of equivalent diameter, (a) non-spherical particle, (b) spherical particle.

Defining a characteristic dimension does not make a non-spherical particle behave like a rigid sphere. Equivalent diameter helps us in mathematical derivation. However, this derivation should be done in order to express the behavior of the non-spherical particle. Therefore, we need more reasons to assume the particle as a rigid sphere. Many researches on fluid dynamic and colloidal science say that particles rotate when they fall. This rotation is obviously caused by a difference in the surface shear stress between the side facing the other particle and the outside (Wu and Manasseh 1998). As a result of rotation, particle's shape could be considered as a sphere. This is shown in Figure 3.2. and also a reason for the equivalent diameter.

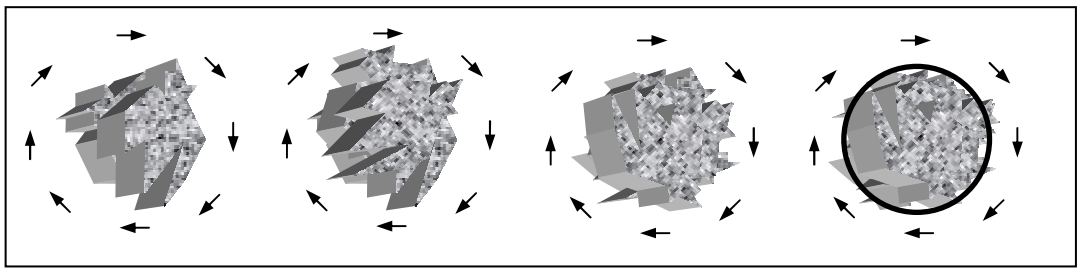

Figure 3.2. Schematic explanation of rotation of particle

Moreover; there is one more reason to consider the particle a rigid sphere. This reason deals with the boundary layer. When a body is submersed in a flowing fluid, there exists a boundary layer around the body. The shape of the boundary layer is based on the body's shape and also fluid characteristics. Figure 3.3 illustrates the boundary layer formation. The particle behaves as its boundary layer.

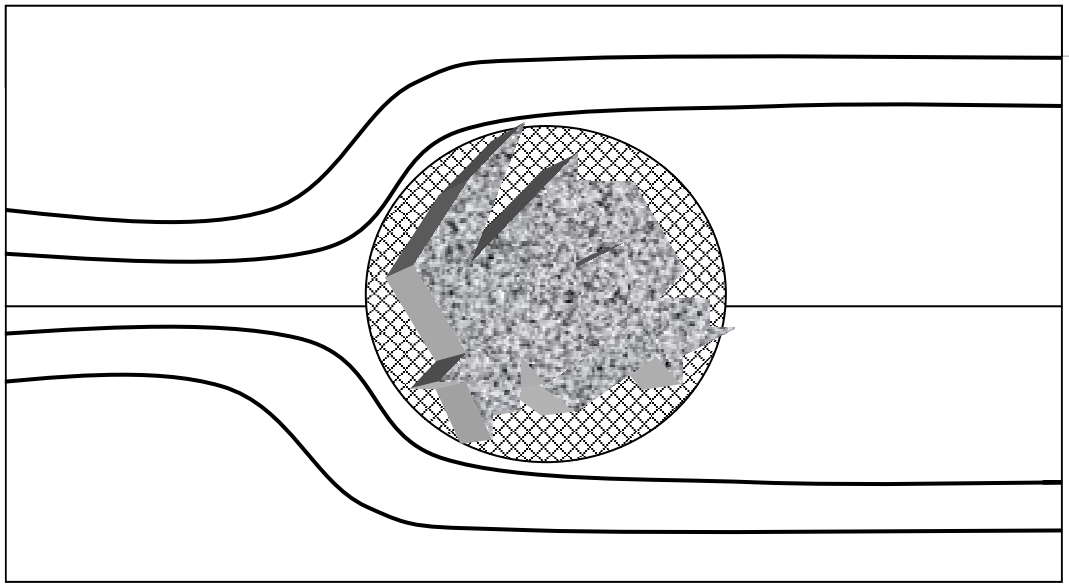

Figure 3.3. Schematic illustration of boundary layer formation

Rough structure of particle's surface disappears with boundary layer formation. As a result of boundary layer formation the non-regular shape can be considered as a sphere.

Particles do not travel lonely. They tend to form an agglomeration. However, many modeling studies consider the particles single. To construct a model with single particles is not a good approach in order to express the real behavior of them. This study

is different at this point. There were some researches in order to prove the agglomeration of the particles (Polat et al. 2002). Polat et al. carried out an experiment. They used a Fresh Dust Generator in order to produce dust particles. A light scattering size measurement device was used to the measure the size of dust particles. This experiment was done twice. Firstly, measurement was done with the particles in air. The particles were dispersed in water for second measurement. Mean size of particles in air was about 20μm while the mean size of the particles in water is about 7 μm. The schematic illustration of these measurements is illustrated in Figure 3.4. Although measurements had done on the same particles, the results were different. This difference is the proof of agglomeration. The particles were agglomerated when they were in air. However, the agglomerates are broken up when they are suspended in water.

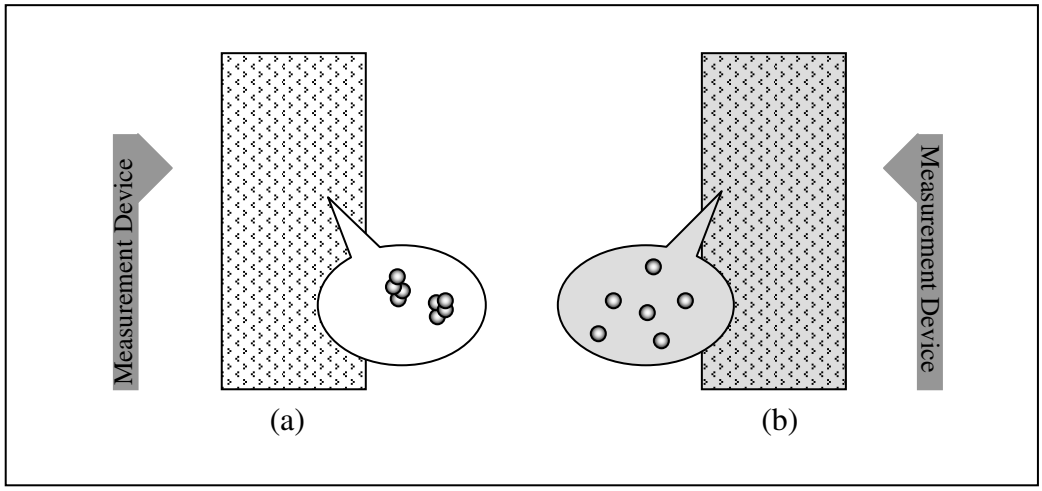

Figure 3.4. Schematic illustration of experiment for determination of particle size (a) Particles in air (b) particles suspended in water.

Particles have been considered single in all the modeling studies about collection of the particles in air. Agglomerated form of non-spherical particles is illustrated in Figure3.5.

Agglomerated geometry is not a regular geometry like non-spherical particles. The shape simplification can be applied on the agglomerated form (See Figure 3.1, 3.2, and 3.3). Size of the agglomerated non-spherical particle will be bigger than non-spherical particles. As a result of these approaches; a equivalent diameter will be used for non-spherical particles and this radius is multiplied by 3 for agglomeration. The number three is the result of the experiment (Polat et al. 2002).

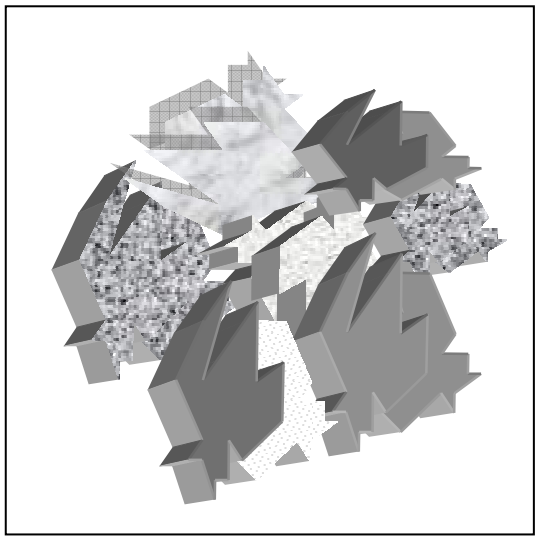

Figure 3.5. Schematic illustration of agglomerated non-spherical particles

3.2. Collision

There are three important particle capture procedures between particle and droplet. These are collision, adhesion and engulfment procedures as mentioned in previous title. Collision is the first interaction between particle and droplet. If the external and inertial forces on the bodies is forced them to each other, collision will occur. Therefore, these forces must be discussed in order to understand collision.

In this study, the problem is if collision occurs between a dust particle and a liquid droplet. Firstly, impaction mechanisms must be explained between these macroscopic bodies. There are five impaction mechanisms between macroscopic bodies under potential flow conditions. These are interception, inertia impaction, diffusion, sedimentation and electrostatic attraction. If there was a collision between a droplet and a particle, one or more of these mechanisms would be effective.

Particles travel through the streamlines around the droplets. Interception occurs when the particles do not depart from the streamlines. Particles neglect their inertia and follow the way of streamlines such as arcuation. Particles following streamlines may arrive at the droplet and get intercepted on the droplet surface. The interception is illustrated in Figure 3.6.

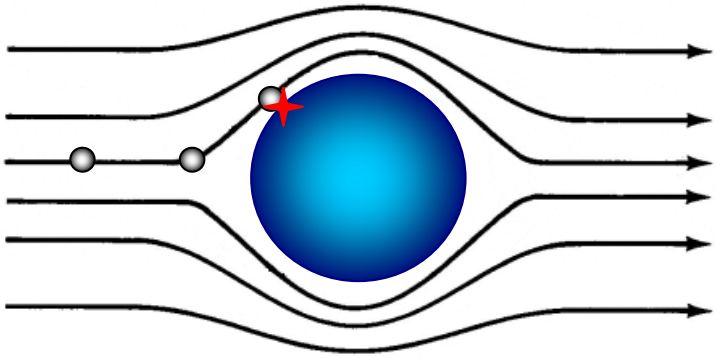

Figure 3.6. Schematic illustration of interception

Inertial impaction occurs when the inertia of the particle is not negligible. The particle may not adjust itself to the sudden change of the streamlines near the droplets. The particle will depart from the streamline and impact on the droplet surface. Figure 3.7. shows the inertia impaction.

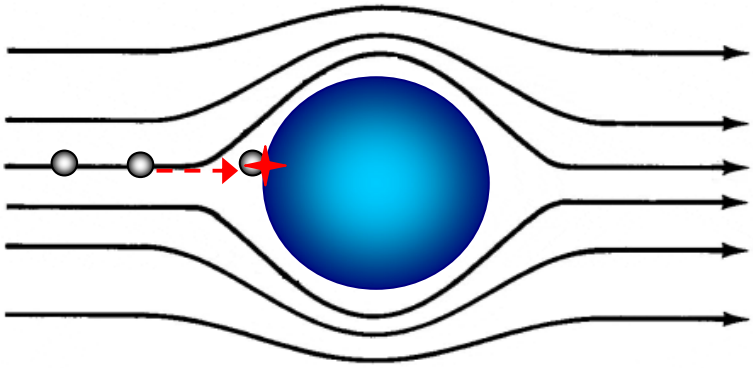

Figure 3.7. Schematic illustration of inertia impaction

Diffusion is another impaction mechanism due to the Brownian motion of the particles. Brownian motion means random moves of the object. It is a hard work to model the Brownian motion. A particle may impact on the surface of the droplet while its Brownian motion as it is shown in Figure 3.8.

The one of the most important force on the earth is the gravitational force. Gravity will affect the particle like all the other objects. Particle may settle by gravitation. An impaction may occur while sedimentation, as it is shown in Figure 3.9.

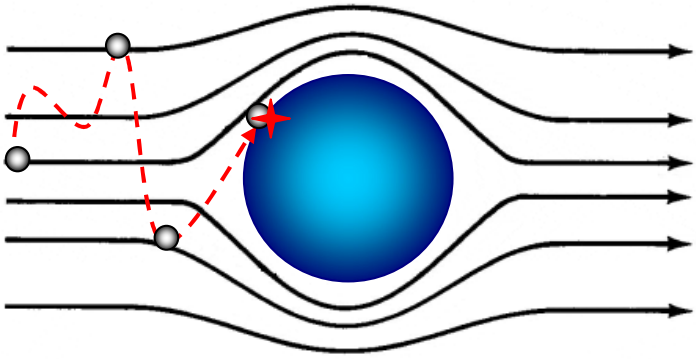

Figure 3.8. Schematic illustration of diffusion

Particle and droplet have electrical charges due to their atomic or molecular structure. There might be an attractive force between particle and droplet due to the electrical charges. This type of impaction is called electrostatic interaction and it is shown in Figure 3.10.

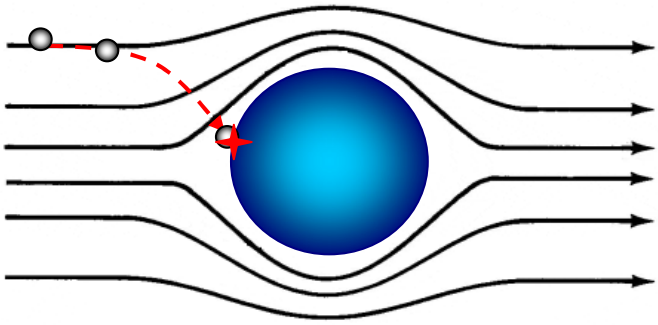

Figure 3.9. Schematic illustration of sedimentation

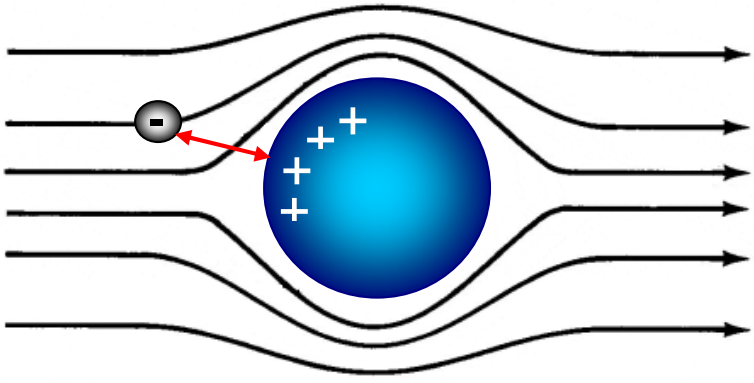

Figure 3.10. Schematic illustration of electrostatic interaction

All the impaction mechanisms are the results of the body forces. If there was no force on the particle, then the particle would not tend to move in these ways. These forces can be classified in two main groups that are external and internal forces. External forces are gravitational force and drag force. Gravitational force is due to the gravitational acceleration and the mass of the body. However; drag force is more complicated than gravitational force. Shape of the particle and the uniform flow rate of the fluid and also the type of the fluid are the components of the drag force. Moreover; internal forces are due to the physical, electrical, chemical and magnetic properties of the matter. The external condition and situation do not affect the internal forces. The most important internal force action on the body is Van der Waals Forces. Van der Waals interaction is due to the dipole moment of the atoms or molecules. The second internal force is electrostatic force due to the electrical behavior of the body. There are also other internal and external forces such as steric forces lift force on the body but they are not as important as the ones just mentioned above.

All the forces acting on the bodies are not always effective on the system. Sometimes, the internal forces are dominant while some other times external ones become dominant. The system dynamics and situation determine which forces are effective. The main problem is if collision occurs due to the all five impaction mechanisms and all the internal and external forces acting on the bodies. All the collision mechanism won't be effective on the system. Diffusion is a complex mechanism to model due to Brownian motion. There are several parameters effective on this mechanisms and this random motion of the particles should be neglected. Electrostatic interactions are the second neglectable mechanism for collision since the electrostatic properties of the particles is hard to quantify. Electrostatic interactions and diffusion must be considered as they have no effect on the system. Sedimentation, inertia impaction and interception must be considered as effective mechanism on collision. Also these three mechanisms are the results of the external forces. The distance between particle and droplet is huge with respect to their sizes when collision occurs. There will be no contact before collision. Internal forces such as Van der Waals and electrostatic forces are effective when the distance between bodies are so small. Therefore, internal forces will be assumed as they do not exist for collision. As a conclusion, external forces are effective on collision whereas the internal forces are neglected. Interception, inertia impaction and sedimentation will be the impaction mechanisms due to the external forces.

Sedimentation is the result of gravitational force as mentioned before. However, there must be additional external forces for inertia impaction and interception. Drag force due to the uniform flow causes the inertia impaction and interception mechanism. The resultant force on the body will conclude the path way of the particle and also droplet. If the pathways of the bodies are crossed then the collision occurs between then. Here is a different approach is needed to solve the system. Figure 3.11 shows all the forces on a particle when uniform flow rate is in positive x direction. The flow rate's direction may be different and so the drag force will be in different directions.

Velocity components of the particle or droplet can be found by momentum balance on it. Momentum balance in x, y and z direction will give all the components of the velocity and location of the bodies.

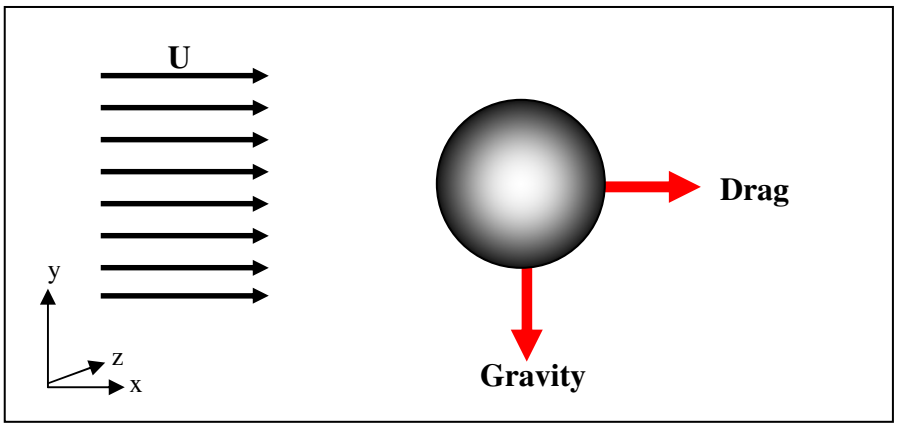

Figure 3.11. External forces on a spherical body when U is in (+)*x* direction

Momentum balance in *X* direction:

All the forces in x direction must be included to momentum balance. If there is flow in x direction, then there exists only drag force. The momentum balance will be:

$$\underbrace{m.\frac{du_x^p}{dt}}_{\text{Net force in x direction}} = \underbrace{\frac{3\pi\mu d}{C_c}\left(u_x^f - u_x^p\right)}_{\text{Drag force in x direction}} \tag{3.2}$$

where u_x^p is the velocity of the particle in x direction and u_x^f is the uniform flow rate is in x direction. Divide both sides of the Eq. 3.2 with $\frac{3\pi\mu d}{C_c}$.

$$\frac{mC_c}{3\pi\mu d}\frac{du_x^p}{dt} = u_x^f - u_x^p \tag{3.3}$$

$$\frac{mC_c}{3\pi\mu d} = \tau \text{ (•)} \tag{3.4}$$

$$\tau \frac{du_x^p}{dt} = u_x^f - u_x^p \tag{3.5}$$

$$\tau \frac{du_x^p}{dt} + u_x^p = u_x^f \text{ (O.D.E)} \tag{3.6}$$

Eq. 3.6 is an ordinary differential equation. The solution of it contains homogeneous and particular solution. Solution of this ordinary differential equation is:

Homogenous Solution

Assume that Eq. 3.6 is homogeneous:

$$\tau \frac{du_x^p}{dt} + u_x^p = 0 \tag{3.7}$$

Assume that:

$$u_x^p = e^{rt} \tag{3.8}$$

Apply Eq. 3.8 to Eq. 3.7.

$$\tau.r.e^{rt} + e^{rt} = 0 \quad \Rightarrow \quad r = -\frac{1}{\tau} \tag{3.9}$$

Finally, homogeneous solution is:

$$u_x^p = C_1 e^{-\frac{t}{\tau}} \tag{3.10}$$

Particular Solution

Assume that particular solution of u_x^p :

$$u_x^p = C_2 \tag{3.11}$$

Apply Eq. 3.11 to Eq. 3.6:

$$C_2 = u_x^f \tag{3.12}$$

$$u_x^p = u_x^p(\text{hom}\,ogeneous) + u_x^p(particular)$$

$$u_x^p = C_1.e^{-\frac{t}{\tau}} + u_x^f \tag{3.13}$$

• Program line (26 and 34) in APPENDIX C

Boundary Conditions

- t=0 $\Rightarrow$ $u_x^p = 0$ then $C_1 = -u_x^f$ (3.14)

Finally, the velocity is in x direction is:

$$u_x^p = u_x^f.(1 - e^{-\frac{t}{\tau}}) \tag{3.15}$$

Location of the particle can be found by integrating the velocity function of it with respect to time. By integrating the Eq. 3.15 the velocity component can be found.

$$x^p = \int u_x^p dt \tag{3.16}$$

$$x^p = \int u_x^f.(1 - e^{-\frac{t}{\tau}})$$

$$x^p = u_x^f \left(t + \tau.e^{-\frac{t}{\tau}} \right) + C_3 \tag{3.17}$$

Boundary Conditions

- t=0 $\Rightarrow$ $x^p = 0$ then $C_3 = -u_x^f \tau$ (3.18)

Finally, the displacement in *x* direction when the uniform flow is in positive *x* direction will be:

$$x^p = u_x^f \tau \left[\frac{t}{\tau} - 1 + e^{-\frac{t}{\tau}} \right] \tag{3.19}$$

When the uniform flow is in negative *x* direction, it will be:

$$x^p = -u_x^f \tau \left[\frac{t}{\tau} - 1 + e^{-\frac{t}{\tau}} \right] \quad (\bullet) \tag{3.20}$$

Momentum balance in *Y* direction:

In contrast to *x* direction gravitational force must be added to momentum balance in this direction. The gravitational force is in negative *y* direction. Let use assume that the flow is in negative y direction like gravitational force.

$$\underbrace{m.\frac{du_y^p}{dt}}_{\text{Net force in y direction}} = \underbrace{\frac{3\pi\mu d}{C_c}\left(u_y^f - u_y^p\right)}_{\text{Drag force in y direction}} + \underbrace{mg}_{\text{Gravitational force}} \tag{3.21}$$

• Program line (38 and 45) in APPENDIX C

Where u_y^p is the velocity of the particle in x direction and u_y^f is the uniform flow rate is in negative *y* direction. Divide both sides of the Eq. 3.21 with $\frac{3\pi\mu d}{C_c}$.

$$\frac{mC_c}{3\pi\mu d}\frac{du_y^p}{dt} = u_y^f - u_y^p + \frac{mC_c g}{3\pi\mu d} \tag{3.22}$$

$$\tau\frac{du_y^p}{dt} = u_y^f - u_y^p + \tau g \tag{3.23}$$

$$\tau\frac{du_y^p}{dt} + u_y^p = u_y^p + \tau g \text{ (O.D.E.)} \tag{3.24}$$

Eq. 3.24 is an ordinary differential equation. The solution of it contains homogeneous and particular solution. Solution of this ordinary differential equation is:

Homogenous Solution

Assume that Eq. 3.24 is homogeneous:

$$\tau\frac{du_y^p}{dt} + u_y^p = 0 \tag{3.25}$$

Assume that:

$$u_y^p = e^{r.t} \tag{3.26}$$

Apply Eq. 3.26 to Eq. 3.25:

$$\tau.r.e^{rt} + e^{rt} = 0 \quad \Rightarrow \quad r = -\frac{1}{\tau} \tag{3.27}$$

Finally, homogeneous solution is:

$$u_y^p = C_4 e^{-\frac{t}{\tau}} \tag{3.28}$$

Particular Solution

Assume that particular solution of u_y^p :

$$u_y^p = C_5 \tag{3.29}$$

Apply Eq. 3.29 to Eq. 3.24:

$$C_5 = u_y^f + \tau g \tag{3.30}$$

$$u_y^p = u_y^p(\text{hom}\,ogeneous) + u_y^p(particular)$$

$$u_y^p = C_4.e^{-\frac{t}{\tau}} + u_y^f + \tau g \tag{3.31}$$

Boundary Conditions

- t=0 $\Rightarrow$ $u_y^p = 0$ then $C_4 = -(u_y^f + \tau g)$ (3.32)

Finally, the velocity is in *y* direction is:

$$u_y^p = (u_y^f + \tau g).(1 - e^{-\frac{t}{\tau}}) \tag{3.33}$$

Location of the particle can be found by integrating the velocity function of it with respect to time. By integrating the Eq. 3.33 the velocity component can be found.

$$y^p = \int u_y^p dt \tag{3.34}$$

$$y^p = \int (u_y^f + \tau g).(1 - e^{-\frac{t}{\tau}})dt$$

$$y^p = (u_x^f + \tau g)\left(t + \tau.e^{-\frac{t}{\tau}}\right) + C_5 \tag{3.35}$$

Boundary Conditions

- t=0 $\Rightarrow$ $y^p = 0$ then $C_5 = -(u_y^f + \tau g)\tau$ (3.36)

Finally, the displacement in *y* direction when the uniform flow is in negative *y* direction will be:

$$y^p = (u_x^f + \tau g)\tau\left[\frac{t}{\tau} - 1 + e^{-\frac{t}{\tau}}\right] \tag{3.37}$$

When the uniform flow is in positive *y* direction, it will be:

$$y^p = (u_x^f - \tau g)\tau\left[\frac{t}{\tau} - 1 + e^{-\frac{t}{\tau}}\right] (\bullet) \tag{3.38}$$

Momentum balance in *Z* direction:

Similarly in *x* direction; if uniform flow is in positive *z* direction, the displacement in *z* will be:

• Program line (39 and 46) in APPENDIX C

$$z^p = u_z^f \tau \left[\frac{t}{\tau} - 1 + e^{-\frac{t}{\tau}} \right] \tag{3.39}$$

If flow is in negative z direction, the displacement in z will be:

$$z^p = -u_z^f \tau \left[\frac{t}{\tau} - 1 + e^{-\frac{t}{\tau}} \right] \tag{3.40}$$

3.2.1. Collision Probability by Simulation

According to momentum balance on the particle given in previous section, a computer simulation may be done. Firstly, a controlled volume will be chosen. A certain number of particles and droplets are placed in this control volume randomly. According to flow conditions, diameters of bodies, physical properties of them the particles start to move. The pathways of them are calculated based on the momentum balance in this section. This simulation can be played as a film and also it can give a probability of collision value. The collision probability can be defined as the ratio between numbers of captured particle and number of total particles.

$$P_{collision} = \frac{n_{cap.}}{n_{tot.}} \tag{3.41}$$

Algorithm of the code is given in Figure 3.12 and the program code is given in APPENDIX B and APPENDIX C.

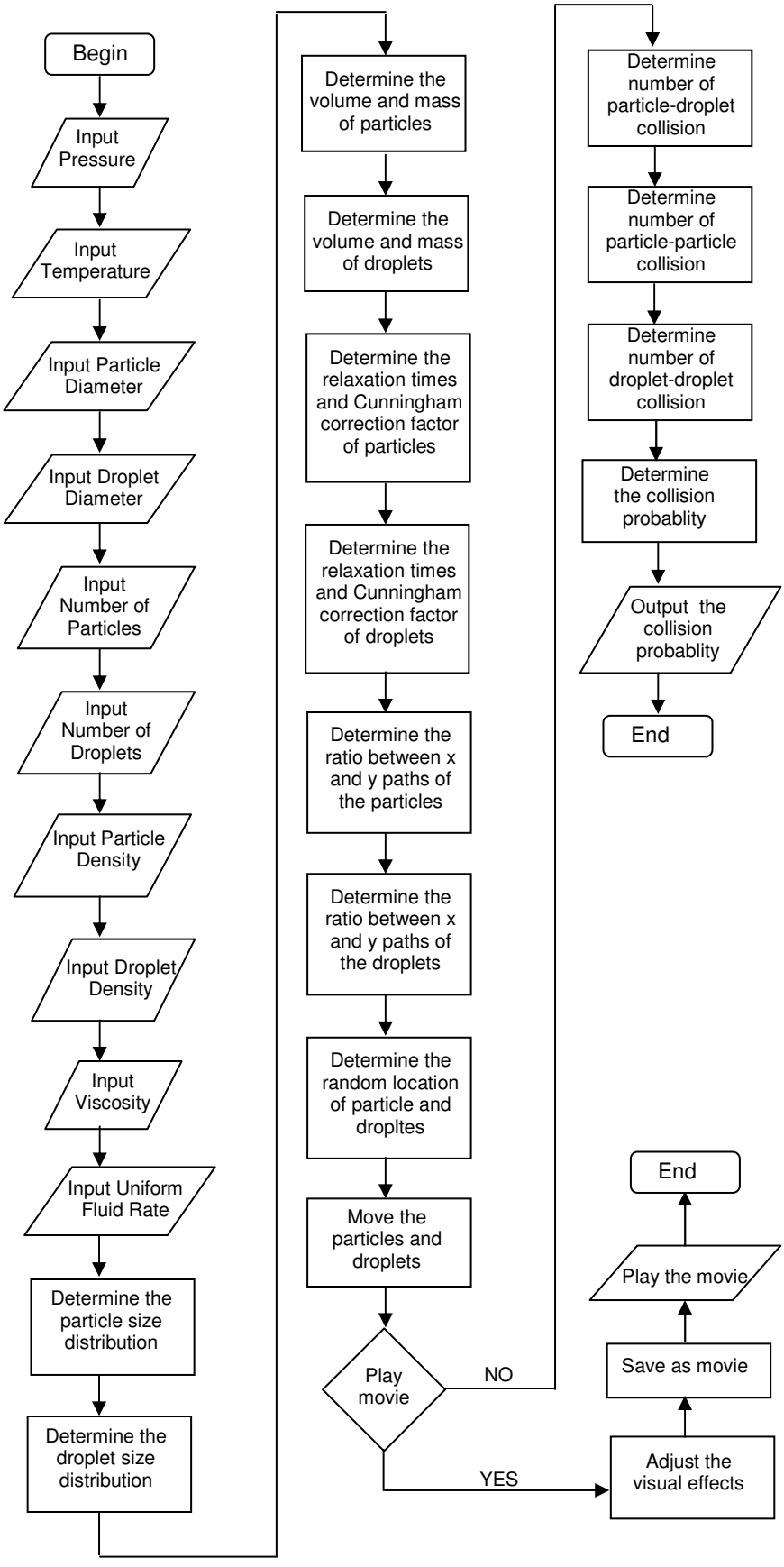

Figure 3.12. Algorithm for movie and collision efficiency code

3.3. Adhesion

Collision is the first mechanism of capturing. However, capturing does not occur by only collision. Two important considerations could be done. One is that particles can be thought as elastic balls and the other is that particles can be thought as adhesive balls. They will repel each other after collision if elastic balls assumption is accepted. However, the balls will join to each other in the other case. As a result of that collision is not the one mechanism to collection of particles. If capturing wants to be achieved adhesion must occur as the second step.

Adhesion is the second important mechanism deals with the adhesive forces. When the particles impact with each other, the distance between them is getting smaller. Therefore, internal forces on the particle will be dominant with this small separation distance. The internal forces will conclude if adhesion occurs. As we mentioned in previous section, the effective internal forces are Van der Waals and electrostatic forces. Enough theoretical background is given in theory section for these forces.

Sum of Van der Waals and Electrostatics forces explains the total internal interaction energy and force between particles. However, this theory generally is applied to aqueous systems.

$$F_{Tot} = F_{VdW} + F_{El} \tag{3.41}$$

$$F_{Tot} = \frac{A_{132}}{6}\frac{R_1 R_2}{H^2(R_1+R_2)} - 2\kappa.e^{-\kappa H}\left[\left(\frac{2\pi.\varepsilon.\varepsilon_0.\kappa.R_1R_2\psi_{01}\psi_{02}}{R_1+R_2}\right)\left(\frac{1}{1-e^{-2\kappa H}}\right)+\left(\frac{\pi\varepsilon.\varepsilon_0.\kappa.R_1R_2(\psi_{01}^2+\psi_{02}^2)}{R_1+R_2}\right)\left(\frac{e^{-\kappa H}}{1+e^{-2\kappa H}}\right)\right] \tag{3.42}$$

Electrostatic interaction part of this equation must be modified for systems in air. The surface potential value and Electrokinetic potential values of the particle are hard to quantify in air. Moreover, the electrical double layer properties will be changed. There is a need to restate the electrostatic interactions.

A new equation must be introduced in order to explain the electrostatic interaction of particles in air (Park and Young 2005). This interaction can be given as:

$$F_{El} = E.q \tag{3.43}$$

where; E is the electrical field and q is the charge of the particle. If there is uniform electrical field in the medium, then the particles tend to move to the plate with opposite

sign according to their electrical charges. However, the title of this study does not cover an electrical field. If there is an electrical filed, it will only be uniform for the experimental setups. Existence of uniform electrical field is not a common situation in real systems. The model dealing with the non-uniform electrical field and its application require serious researches. Moreover, the charge of particle is hard to quantify. One particle can have a positive sign whereas the other is negative. The charge density of the particles won't be equal all the particles in the system. As a conclusion, the electrostatic interactions between particles in air are not a proper job to model. Many data and information could be obtained by experiments however equations are not clear. Electrostatic interactions are also small distance interactions for aqueous medium. At this point, this interaction will be canceled out. The effective force for adhesion is only the Van der Waals force.

$$F_{Ad} = F_{VdW} = \frac{A_{132}}{6} \frac{R_1 R_2}{H^2 (R_1 + R_2)} \tag{3.44}$$

In this study, only Van der Waals interaction will conclude if adhesion occurs. Van der Waals forces generally are attractive forces. Hamaker constant will conclude the sign of this interaction. If Hamaker constant is positive there will be a attraction then adhesion occurs. Otherwise, adhesion does not occur because of the repulsive interaction. In air, there is no possibility for Hamaker constant to be negative. As a result, Adhesion possibility is considered as one.

3.4. Engulfment

The last collection mechanism is engulfment. Engulfment is the about the absorption ability of particles by liquid droplets. If engulfment does not occur, then the collection of particles won't be completed. Collision helps particles and droplets to make closer to each other. Adhesion will conclude if particles are held on the surface of the droplets. However, these mechanisms are not enough for complete collection. Engulfment is the desired last mechanism of collection.

Particles are loaded on the surface of the droplets by adhesion. Excess particle load will limit the adhesion mechanism since there is no available place on the droplet surface to adhesive. Particles must be absorbed by liquid droplets in order to leave free surface on the droplet for adhesion of the other particles. This relation is shown in

Figure 3.13. Decreasing of engulfment possibility will decrease the adhesion. Moreover; engulfment is effective on continuity of adhesion.

Engulfment mechanism deals with Surface tensions of the liquid molecules. The surface tension γ is the magnitude F of the force exerted parallel to the surface of a liquid divided by the length L of the line over which the force acts:

$$\gamma = \frac{F}{L} \tag{3.45}$$

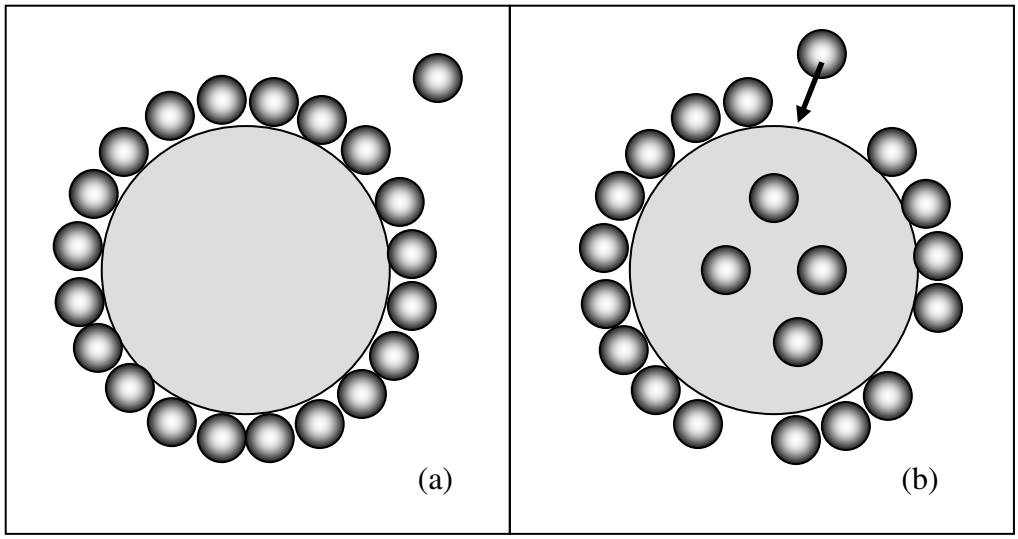

Figure 3.13. Schematic illustrations of engulfment, (a) No engulfment and adhesion does not occur, (b) engulfment occurs and adhesion continuous.

Surface tension of liquid molecules concludes if engulfment occurs. Engulfment probability will be less with liquid droplets with higher surface tension. In order to adjust the surface tension and increase the engulfment ability of the droplets, surfactants molecules can be added to solution. Also surface tension will be changed with temperature. The surface tension for water against the air is summarized in Table 3.1 (Israelachvili 1992).

Table 3.1. Surface tension change with temperature of water against the air.

Temperature (° C)	**Surface Tension (erg cm^{-2})**
-8	77.0
-5	76.4
0	75.6
5	74.9
10	74.22
15	73.49
18	73.05
20	72.75
30	71.18
40	69.56
50	67.91
60	66.18
70	64.4
80	62.6
100	58.9

In this study, addition of surfactant and their effect were not discussed. In order to increase engulfment, proper surfactants could be added to system. However, to model the effects of the surfactant molecules is another field of study. As a conclusion, engulfment probability will be considered as unity.

CHAPTER 4

RESULTS AND DISCUSSION

Particle collection by liquid droplets under potential flow conditions was modeled in this study. There are three important collection mechanisms such as collision, adhesion and engulfment. Collision probability was calculated by simulation while adhesion and engulfment probabilities were decided by appropriate equations. This study was focused on collision probability. Collisions were the result of gravitational and drag forces. Simulation was made and inputs of the program were determined according to these forces. Particle number, droplet number, particle diameter, droplet diameter, uniform flow velocity and density of the particles were chosen as effective parameters. The effects of these parameters on collision probability were discussed firstly. In order to discuss each parameter, all the other parameters were kept constant and only the parameter changed at a time.

Particle number is concern with particle concentration. An increase is expected on collision probability when particle number is increased. However, there is no proportionality between collision probability and particle number as it is seen in Figure 4.1. Collision probability remains unchanged when particle number is increased. This is thought as an unexpected situation. But, collision efficiency is explained by the ratio between number of captured particles and number of all particles in the control volume. An increase in number of particles is resulted in an increase in number of captured particles. Hence, the ratio, collision probability, remains constant.

Droplet number is concern with droplet concentration such as collector concentrations (mg/m^3). More collision is achieved with increasing in collector numbers. This expected situation is observed as it is seen in Figure 4.2. In order to increase the collision probability, the droplet number can be easily increased. However, cost of the method is increased. An optimization should be done on the system in order to minimize the cost and maximize the collision efficiency.

Particle diameter is an important parameter for health problems as it is mentioned in introduction. A certain size range is achieved to be captured. Figure 4.3. shows the effect of particle diameter on collision efficiency. Collision probability is increased with increasing particle diameter as it is seen easily in related figure. This

relation could also be explained by increase of gravitational force on the particles. The acceleration of particles will be higher than droplets. Variations in velocity of particles and droplets are resulted in more collision. Moreover, bulk concentration of particles increases with the increasing of particle diameter. An increase in collision efficiency is expected with higher bulk concentration of particles.

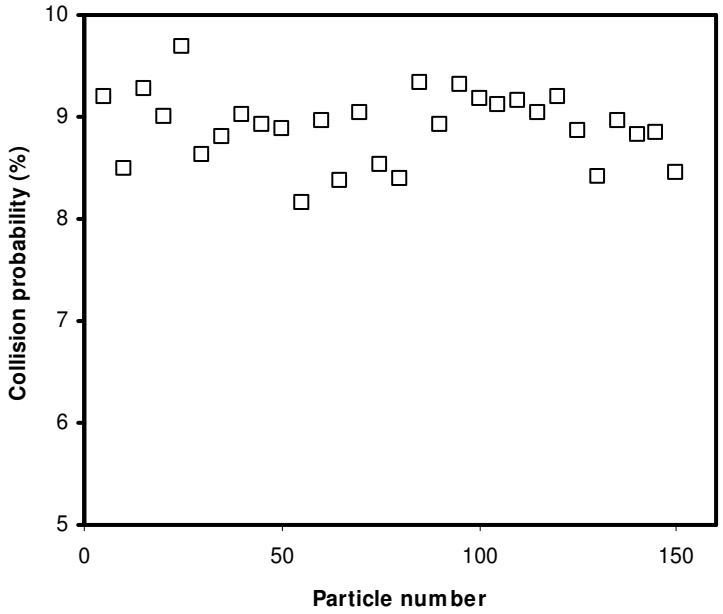

Figure 4.1. Collision probability as a function of particle number when # of droplets=70, particle diameter=5μm, droplet diameter=10μm, density of particle=2600kg/m^3, uniform flow velocity=10m/s.

Similarly, droplet diameter is concern with droplet concentration (mg/m^3) such as collector concentration. The collision probability is expected to increase when bigger collectors are introduced to the control volume. The relation between collision probability and droplet diameter is given in Figure 4.4. An increase in droplet diameter resulted in increase of bulk concentration of droplets. The cost will be strongly influenced by increase in bulk concentration of droplets. As a conclusion, an optimization should be done on droplet diameter.

Drag force is the result of uniform flow rate. Drags on both droplets and particles are influenced by the change of uniform flow velocity. Both of the bodies tend to accelerate when the flow rate is increased whereas they tend to decelerate when the flow rate is decreased. There will be no relative difference between velocities of the

bodies. Finally, any important chances on collision efficiency are not expected by changing the uniform flow rate as can be seen in Figure 4.5.

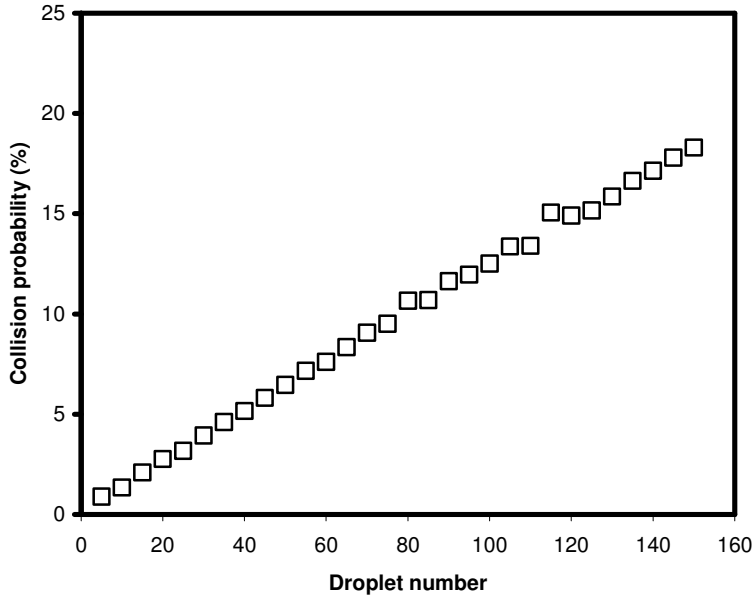

Figure 4.2. Collision efficiency as a function of droplet number when # of particles=70, particle diameter=5μm, droplet diameter=10μm, density of particle=2600kg/m^3,uniform flow velocity=10m/s.

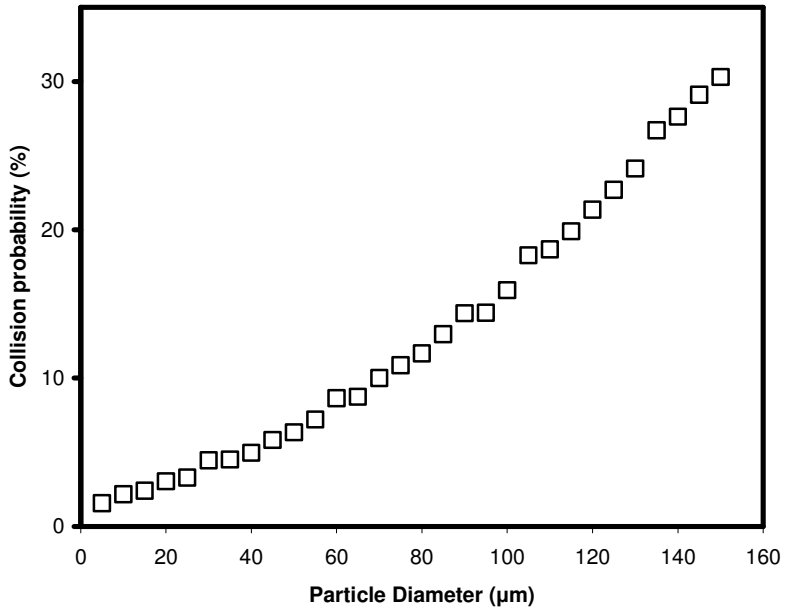

Figure 4.3. Collision efficiency as a function of particle diameter when # of particles=70, # of droplet=70, droplet diameter=10μm, density of particle=2600kg/m^3,uniform flow velocity=10m/s.

Particle density is the last parameter will be discussed on the collision mechanism. Density of a particle will affect the gravitational force. If gravitational force on a particle is increased, then the acceleration in negative *y* direction will increase. The particles show a tendency to remove the control volume rapidly according to droplets. At this point, collision efficiency is expected to show a decrease with increasing particle density. However, particles may be impact with the droplets that in the below control volume. As a conclusion, the collision probability is not affected by particle density as it is seen in Figure 4.6.

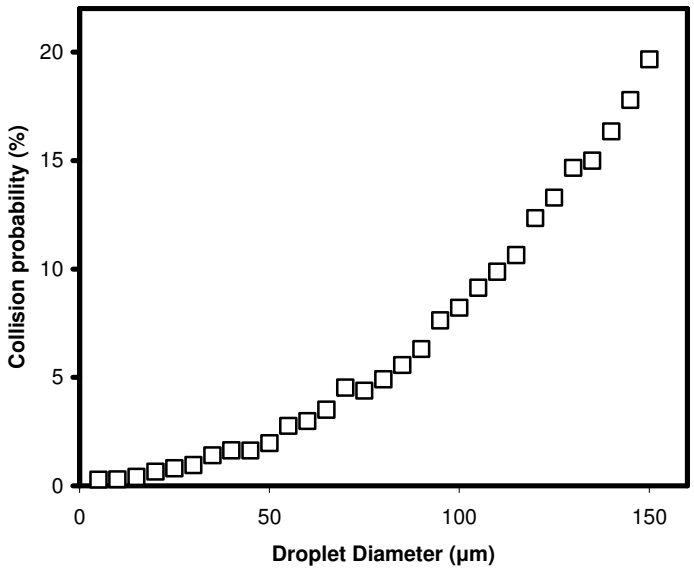

Figure 4.4. Collision efficiency as a function of particle diameter when # of particles=70, # of droplet=70, particle diameter=5µm, density of particle=2600kg/m^3,uniform flow velocity=10m/s.

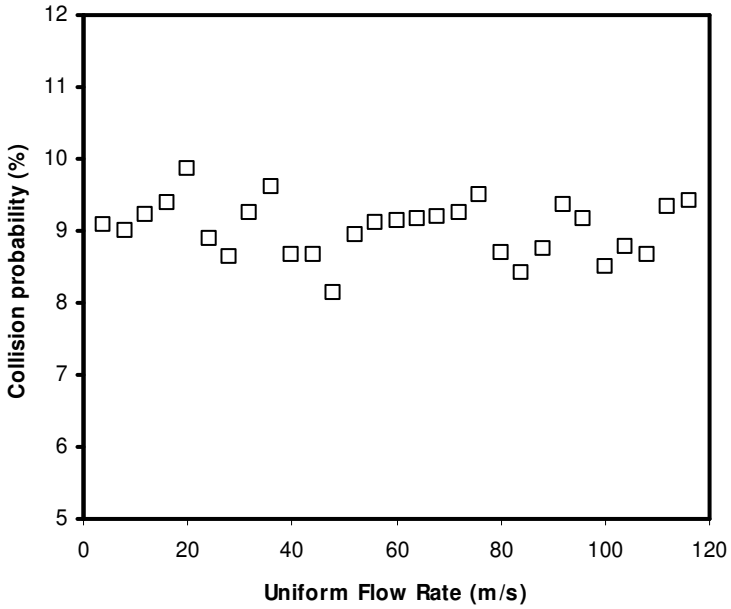

Figure 4.5. Collision efficiency as a function of uniform flow rate when # of particles=70, # of droplet=70, particle diameter=5μm, droplet diameter=10 μm, density of particle=2600kg/m^3.

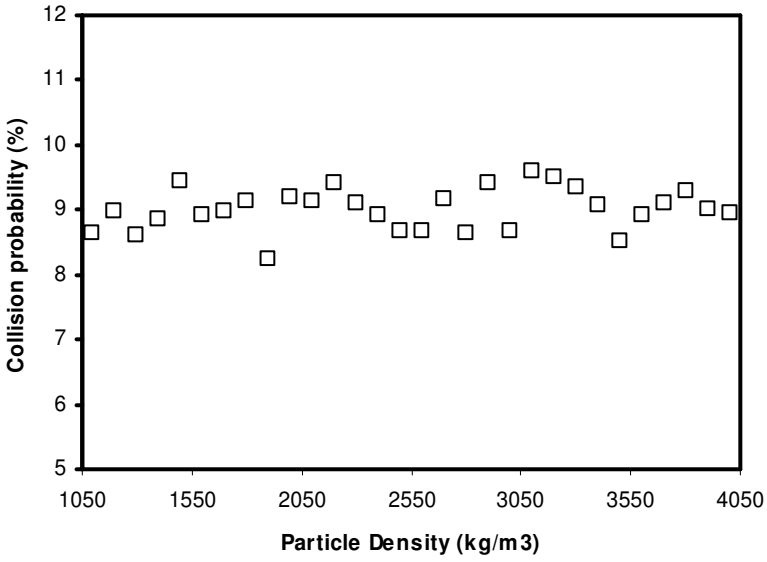

Figure 4.6. Collision efficiency as a function of density of particle when # of particles=70, # of droplet=70, particle diameter=5μm, droplet diameter=10 μm, uniform flow rate=10m/s.

Six important parameters on collision mechanism were discussed. As shown in the figures, uniform flow velocity and particle density had no effect on collision mechanism strongly. Other parameters deal with particle and droplet bulk concentrations. During calculations, a certain parameter's influence on collision mechanism is investigated by varying the level between a certain range, and keeping all the other parameters' level constant. Simulations were also carried out to see interaction between parameters and with that of the collision probability using a three-level, full factorial design of experiment matrix. The surface plots of this design are given in Figure 4.7. and Figure 4.8. There are proportionalities in surface plots and singles plots as it is seen in figures.

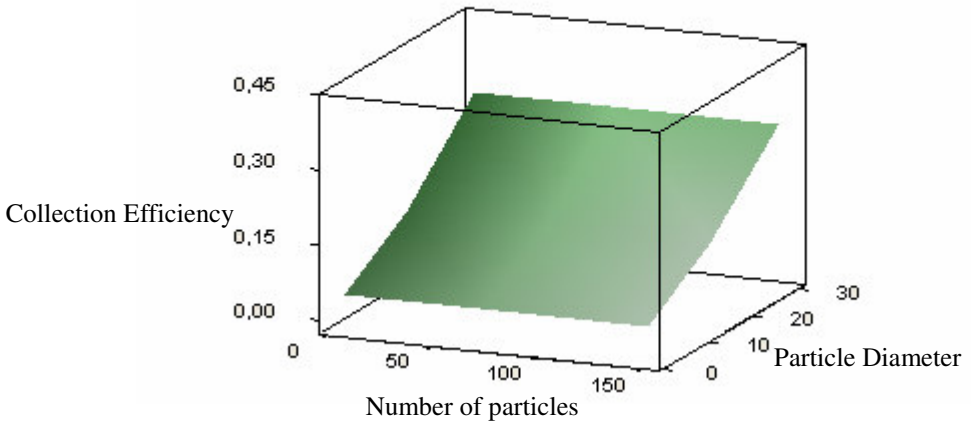

Figure 4.7. Surface plot of collection efficiency with respect to number of particles and particle diameter.

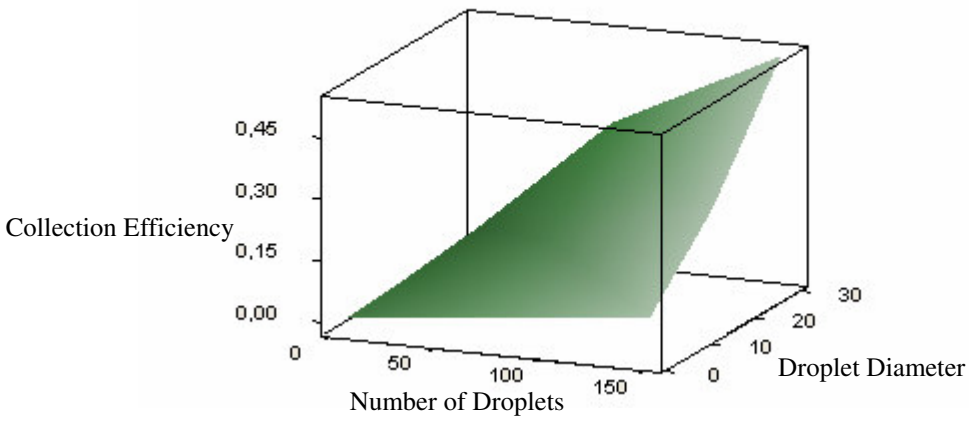

Figure 4. 8. Surface plot of collection efficiency with respect to number of droplets and particle droplets.

Collision mechanism was discussed. There are also two important mechanisms such as adhesion and engulfment. Adhesion is assumed as a result of Van der Waals interaction in this study. Van der Waals forces are usually attractive. Van der Waals forces shows repulsive behavior when the medium's Hamaker constant is between the Hamaker constants of the droplet and particle. The medium is air and its Hamaker constant is nearly zero. Hence, there will be no system in air with repulsive Van der Waals interactions. Van der Waals interaction is assumed always positive in air and probability value will be accepted as one. Engulfment is another important collection mechanism. It is about the particle absorption ability of the liquid droplet. If surface tension of the liquid droplet is reduced, then the engulfment probability is increased. In order to adjust the surface tension of droplets, surfactant can be added to the liquid. Water engulfment ability can be increased by adding the proper surfactants such as Triton X-100 and Aerosol-OT. However, addition of surfactant molecules increases the cost of the method. An increase in engulfment probability will result in increase of adhesion probability because there exists free space on the droplet surface to adhesion after engulfment. This study is focused on the Collision mechanism. A more accurate model that considers adhesion and engulfment can be developed by carrying out experiments. In this study, the probability of adhesion and engulfment were considered to be equal to one. Thus, the collection probability equals to collision probability.

There are several models about collection mechanism of particles by liquid droplets. One of the most important one is Calvert model. Compression should be done Calvert model and the model developed in this study. The models are also compared and discussed with the experimental data. There have been many experimental studies in this literature (Goldshmid and Calvert 1963). Sulphur and polystyrene particles collection efficiency was tested by Goldshmid and Calvert. Water droplets were used as collector. The drops were supported on horizontal hypodermic tubing by an upward-flowing air stream laden with aerosol. Then air stream were analyzed. After experiment, the drops were diluted in flasks and counted in microscope. Particle size was determined by taking the pictures under the microscope (970x). Results are shown in Figure 4.9 for 2.9μm sulphur particles and, in Figure 4.10 for 2.85μm Polystyrene particles.

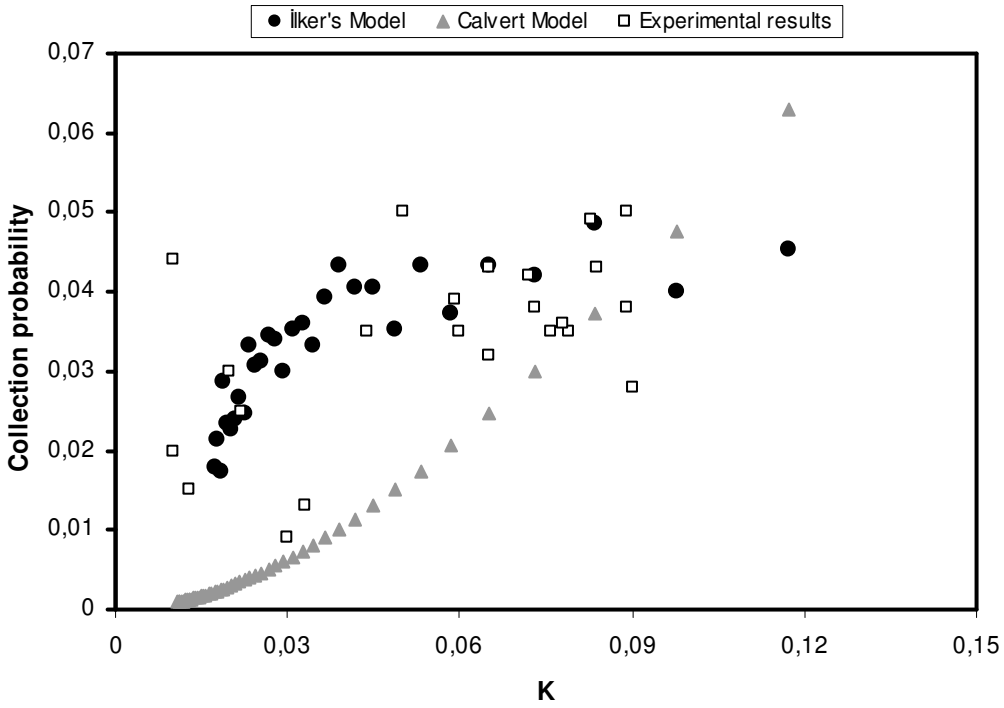

Figure 4.9. Collection probability of 2.9µm Sulphur particles.

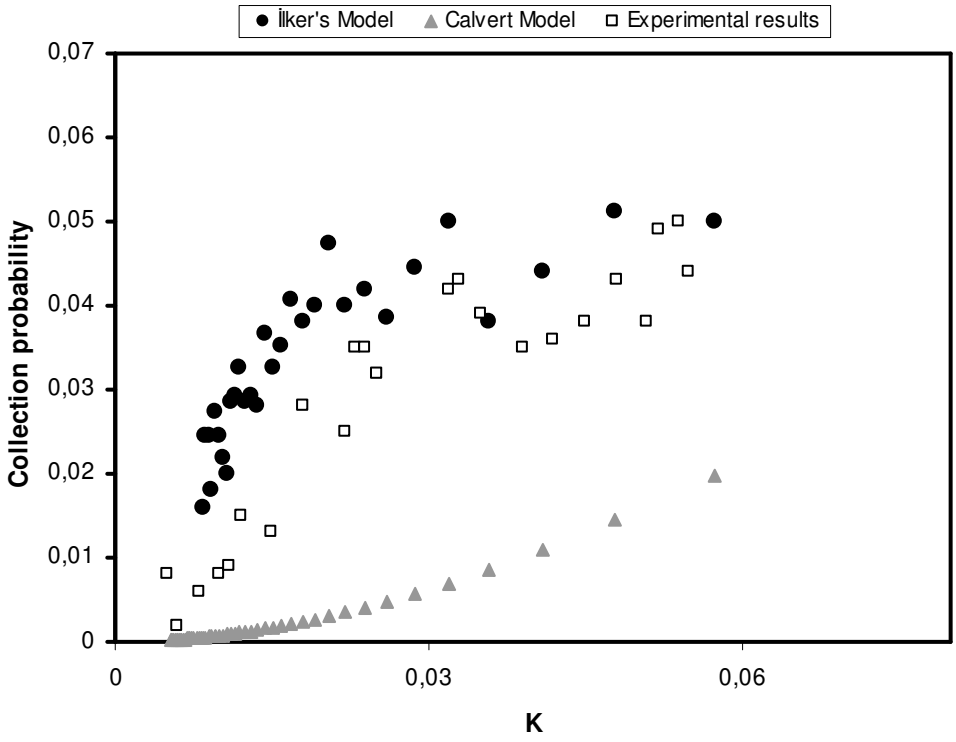

Figure 4.10. Collection probability of 2.85µm Polystyrene particles.

Experimental results show randomness similarly the model was developed in this study. However, Calvert model does not show any random behavior. At this point the model I developed in this study has more similarities with the experimental data compared to Calvert model. Calvert model was calibrated with a constant in order to express the collection efficiency, in my study; no calibration constant was used in the model. Similar results were obtained when the impaction parameter, K, is nearly equal to 0.075.

Although, the model developed in this study gives appropriate results, it should be modified in order to reduce the error coming from the assumptions. The collection efficiency can be affected by non-spherical shape of the particles. Particles can have the same equivalent diameter. However, collection efficiency of a particle with a sharp shape will be different than a particle having smooth surface. Collection mechanisms can also be affected by electrostatic interactions. This interaction should be taken into account. Lift force, structural forces, and steric forces are the most important forces acting upon the particles and droplets. A proper model can be developed by reducing the assumptions, and conducting experiments.

CHAPTER 5

CONCLUSIONS & RECOMMENDATIONS FOR FUTURE STUDIES

A model was developed for collection of non spherical particle assemblies under potential flow conditions. Although particles and droplets were assumed as rigid spheres in all the other modeling studies, a model was constructed for non-spherical particles in this study. Diameters of particles were varied due to particles size distribution. Moreover, particle agglomeration was taken into account and equivalent diameters of particles were assumed as three times of its original value. Consistent results were obtained with experimental data. It is shown that particle collection efficiency can be explained better by assuming non-spherical particle assemblies.

Simulation was the way of calculation of collision efficiency. Particles and droplets were placed into the control volume randomly for each run. Simulation showed more consistency with the experimental data when compared to the other analytical models in the literature such as Calvert model. Application of the equations by computer programming will give more realistic results than the model solely described by an analytical equation.

General results were also obtained through the modeling in this study. Collision probability increases by the increase in the particle diameter. Collision efficiency was higher with bigger particles. Droplet diameter and number are the effective parameters on the collision mechanisms. Collision efficiency increased by increasing droplet diameter. Moreover, there were proportionality between droplet number and collision efficiency. It can be concluded that droplet diameter, particle diameter and number of droplets are the parameters that are the most influential on collision mechanism. Van der Waals interactions led to adhesion of the particles. If overall Hamaker constant is positive there will be an attraction due to the Van der Waals interactions. Otherwise, there will be repulsion. Adhesion occurs when there is an attractive interaction. Engulfment is the mechanism about absorption ability of the droplets. Engulfment ability is concluded by surface tension of the droplets. Engulfment probability is increased by a decrease in surface tension value. Surfactants can be added to the

solution in order to decrease surface tension and increase the engulfment ability of the droplets.

This study is preliminary step of modeling of collection of non-spherical particle assemblies by liquid droplets under potential flow conditions. In order to develop more realistic and proper model, experimental studies should be carried out. Three different collection mechanisms should be investigated in more detailed. The model developed in this study gives a general view about collection mechanisms of particles by liquid droplets.

REFERENCES

Chander, S., Alaboyun, A. R. and Aplan, F. F., 1991. "On the Mechanisms of Capture of Dust Particles by Sprays", 3rd Symposium on Respirable Dust in the Mineral Industries, Eds. R. L. Franz and R. V. Ramani, SME, Littleton, CO.

Concha, F., Almedra, E. R., 1979. "Settling Velocities of Particulate Systems, 1. Settling Velocities of Individual Spherical Particles", *International Journal of Mineral Processing.* Vol. 5, pp. 349-367.

Concha, F., Almedra, E. R., 1979. "Settling Velocities of Particulate Systems, 2. Settling Velocities of Suspensions of Spherical Particles", *International Journal of Mineral Processing*. Vol. 6, pp. 31-41.

Concha, F., Barrientos, A., 1982. "Settling Velocities of Particulate Systems, 3. Power Series Expansion for the Drag Coefficient of a Sphere and Prediction of the Settling Velocity", *Journal of Mineral Processing*. Vol. 9, pp. 167-172.

Concha, F., Barrientos, A., 1986. "Settling Velocities of Particulate Systems, 4. Settling of Non-Spherical Isometric Particles", *International Journal of Mineral Processing.* Vol. 18, pp. 297-308.

Concha, F., Christiansen, A., 1986. "Settling Velocities of Particulate Systems, 5. Settling Velocities of Suspension of Particles of Arbitrary Shape", *International Journal of Mineral Processing*. Vol. 18, pp. 309-322.

Department of Health and Human Services, 2003. *Handbook for Dust Control in Mining*; Centers of Disease Control and Prevention, IC 9465.

Polat, H., Polat, M., Gürgen, S., 2000. "Recent Developments on the suppression of Respirable Dust Using Water Sprays", *Madencilik.* Vol. 39, No. 1, p. 40.

Gary Leal, L., 1992. *Laminar Flow and Convective Transport Processes*, (Butterworth-Heinemann, New York), p. 152.

Goldshmid, Y., Calvert, S., 1963. "Small Particle Collection by Supported Liquid Drops", *A.I.Ch.E. Journal*. Vol. 9, No. 3, pp. 352-358.

Israelachvili, J., 1992. *Intermolecular & Surface Forces*, (Academic Press, New York), p. 153.

Marchand, P., Holland, O.T., 2003. *Graphics and GUIs with Matlab*, (Chapmann& Hall CRC, New York) USA, p. 152.

Munson, B.R., Young, D.F., Okiishi, T.H., 2002. *Fundamentals of Fluid Mechanics,* (John Wiley, New York), p.323.

Park, H. S., Young Ok Park, 2005. "Simulation of Particle Deposition on Filter in an External Electrical Field" , *Journal of Chemical Engineering*. Vol. 22, No. 2, pp. 303-314.

Polat, M., Polat, H., 2000. "A review of the Theory of Interactions between Particles in Aqueous Media, 2. Van der Waals Interactions", *Ore Dressing*. Issue 3, pp. 21-48.

Polat, M., 1999. "A review of the Theory of Interactions between Particles in Aqueous Media, 1. The Electrical Double Layer", *Ore Dressing*. Issue 2, pp. 7-36.

Polat, M., Polat. H., 2000. "A review of the Theory of Interactions between Particles in Aqueous Media, 3. Electrostatic and Structural Interaction and DLVO Theory", *Ore Dressing*. Issue 4, pp. 1-16.

Polat, H., Polat, M., Chander, S., Hogg, R., 2002. "Characterization of Airbone Particles and Droplets: Relation to Amount of Airbone Dust and Dust Collection Efficiency", *Particle-Particle System Characterization*. Vol. 19, pp. 38-46.

Rudnick, S.N., Koehler, J.L.M., Martin, K.P., Leith, D., Cooper, D.W., 1986. "Particle Collection Efficiency in a Venturi Sucrubber: Comparison of Experiments with Theory", *Environ. Sci. Techno.* Vol. 20, No. 3, pp.237-242.

WEB_1, 2005. CRCD's web site (Clarkson University), 13/12/2005. http://www.clarkson.edu/projects/crcd/site_map.html

Wu, J., Manasseh, R., 1998. "Dynamics of Dual-Particle Settling under gravity", *International Journal of Multiphase Flow*. Vol. 24, pp. 1343-1358.

APPENDIX A

MATLAB CODE FOR POTENTIAL FLOW STREAMLINES

```
s=[]; r=[]; x=[]; y=[]; W=[];
T=[]; TA=[]; TB=[]; TC=[]; TD=[]; TE=[]; TF=[]; TG=[]; TH=[]; TI=[]; TJ=[];
g=[]; gA=[]; gB=[]; gC=[]; gD=[]; gE=[]; gF=[]; gG=[]; gH=[]; gI=[]; gJ=[];
h=[]; hA=[]; hB=[]; hC=[]; hD=[]; hE=[]; hF=[]; hG=[]; hH=[]; hI=[]; hJ=[];

a = input('ENTER THE SPHERE RADIUS (m) = ');          % The radius of the sphere
U = input('ENTER THE UNIFORM FLOW RATE (m/s) = ');    % Uniform flow rate

for i=1:181;                % A loop to change the angle around the sphere form 0 to pi
s(i) = (i-1).*(pi./180); % Angle
for j=1:500                 % A loop to change the radius in the flow regime
r(j)=((a+0.01)+(j*0.01));               % r component
W(i,j)= U*r(j)*((1-((a^2)/(r(j)^2))))*sin(s(i));    % Stream Function
x(i,j)=r(j)*cos(s(i)); % Transformation of cylindrical coordinates to Cartesian coordinates
y(i,j)=r(j)*sin(s(i));     % Transformation of cylindrical coordinates to Cartesian coordinates

if      W(i,j)>1.1 & W(i,j)<2.1   % Stream functions between 1.1 and 2.1
    i.  T=[T;[i,j]];
end

if      W(i,j)>4.1 & W(i,j)<6.1    % Stream functions between 4.1 and 6.1
    i.  TA=[TA;[i,j]];
end

if      W(i,j)>10.1 & W(i,j)<12.1 % Stream functions between 10.1 and 12.1

TB=[TB;[i,j]];
end

if      W(i,j)>14.9 & W(i,j)<16.1  % Stream functions between 14.1 and 16.1
    i.  TC=[TC;[i,j]];
end

if      W(i,j)>25.9 & W(i,j)<27.1  % Stream functions between 25.9 and 27.1
    i.  TD=[TD;[i,j]];
end
```

```
25.  if    W(i,j)>36.9 & W(i,j)<38.1   % Stream functions between 36.9 and 38.1
          i. TE=[TE;[i,j]];
26.  end

27.  if    W(i,j)>46.9 & W(i,j)<48.1   % Stream functions between 46.9 and 48.1
          i. TF=[TF;[i,j]];
28.  end

29.  if    W(i,j)>55.1 & W(i,j)<57.1   % Stream functions between 55.1 and 57.1
          i. TG=[TG;[i,j]];
30.  end

31.  if    W(i,j)>67.9 & W(i,j)<69.1   % Stream functions between 67.9 and 69.1
          i. TH=[TH;[i,j]];
32.  end

33.  if    W(i,j)>80.1 & W(i,j)<82.1   % Stream functions between 80.1 and 82.1
          i. TI=[TI;[i,j]];
34.  end

35.  if    W(i,j)>100.1 & W(i,j)<101.1% Stream functions between 100.1 and
     101.1
          i. TJ=[TJ;[i,j]];
36.  end
37.  end
38.  end

39.  I = size (T,1);                    % To find the stream function location in
     Cartesian coordinates
40.  IA = size (TA,1);
41.  IB = size (TB,1);
42.  IC = size (TC,1);
43.  ID = size (TD,1);
44.  IE = size (TE,1);
45.  IF = size (TF,1);
46.  IG = size (TG,1);
47.  IH = size (TH,1);
48.  II = size (TI,1);
49.  IJ = size (TJ,1);

50.  for i=1:I
51.  for j=1:1
52.  g(i,j)=x(T(i,j),T(i,j+1));
53.  h(i,j)=y(T(i,j),T(i,j+1));
54.  end
55.  end

56.  for i=1:IA
57.  for j=1:1
```

```
gA(i,j)=x(TA(i,j),TA(i,j+1));
hA(i,j)=y(TA(i,j),TA(i,j+1));
end
end

for i=1:IB
for j=1:1
gB(i,j)=x(TB(i,j),TB(i,j+1));
hB(i,j)=y(TB(i,j),TB(i,j+1));
end
end

for i=1:IC
for j=1:1
gC(i,j)=x(TC(i,j),TC(i,j+1));
hC(i,j)=y(TC(i,j),TC(i,j+1));
end
end

for i=1:ID
for j=1:1
gD(i,j)=x(TD(i,j),TD(i,j+1));
hD(i,j)=y(TD(i,j),TD(i,j+1));
end
end

for i=1:IE
for j=1:1
gE(i,j)=x(TE(i,j),TE(i,j+1));
hE(i,j)=y(TE(i,j),TE(i,j+1));
end
end

for i=1:IF
for j=1:1
gF(i,j)=x(TF(i,j),TF(i,j+1));
hF(i,j)=y(TF(i,j),TF(i,j+1));
end
end

for i=1:IG
for j=1:1
gG(i,j)=x(TG(i,j),TG(i,j+1));
hG(i,j)=y(TG(i,j),TG(i,j+1));
end
end

for i=1:IH
for j=1:1
gH(i,j)=x(TH(i,j),TH(i,j+1));
```

```
hH(i,j)=y(TH(i,j),TH(i,j+1));
end
end

for i=1:II
for j=1:1
gI(i,j)=x(TI(i,j),TI(i,j+1));
hI(i,j)=y(TI(i,j),TI(i,j+1));
end
end

for i=1:IJ
for j=1:1
gJ(i,j)=x(TJ(i,j),TJ(i,j+1));
hJ(i,j)=y(TJ(i,j),TJ(i,j+1));
end
end

t = -a:0.1:a;                    % To draw the cross sectional area of the
sphere
z = (((a.^2)-(t.^2)).^(1/2));

plot(t,z,t,-z,g,h,g,-h,gA,hA,gA,-hA,gB,hB,gB,-hB,gC,hC,gC,-hC,gD,hD,gD,-
hD,gE,hE,gE,-hE,gF,hF,gF,-hF,gG,hG,gG,-hG,gH,hH,gH,-hH,gI,hI,gI,-
hI,gJ,hJ,gJ,-hJ) % Plotting the stream lines and their negative values

axis off                         % To adjust the axis property
```

APPENDIX B

MATLAB CODE FOR MOVIE OF PARTICLE DROPLET INTERACTION

```
T = input('ENTER THE TEMPERATURE (K) = ');                          % Temperature
P = input('ENTER THE PRESSURE (atm) = ');                           % Pressure
D_1 = input('ENTER THE PARTICLE DIAMETER (micron) = ');             % Particle Diameter
D_2 = input('ENTER THE DROPLET DIAMETER (micron) = ');              % Droplet Diameter
t_1 = input('ENTER THE NUMBER of PARTICLES = ');                    % Particle Number
t_2 = input('ENTER THE NUMBER of DROPLETS = ');                     % Droplet Number
qp_1 = input('ENTER THE PARTICLE DENSITY (kg/m^3) = ');             % Particle Density
qp_2 = input('ENTER THE DROPLET DENSITY (kg/m^3) = ');              % Droplet Density
VV = input('ENTER THE VISCOSITY OF FLUID X 10^7 (kg/m.s) = ');
% Viscosity of Fluid
U = input('ENTER THE UNIFORM FLUID VELOCITY (m/s) = ');
% Uniform Fluid Velocity
Vis = VV*10^(-7);                                                   % In Order To Transform Viscosity In kg\m.s
pr = P*101325;                                                      % In order To Transforn Pressure in bar
g = 9.8;                                                            % Gravitational Acceleration
L = (23.1*T)/pr;                                                    % Molecular mean free path in gas (nm)
DD_1=normrnd(D_1,((D_1)/10),t_1,1);
DD_2=normrnd(D_2,((D_2)/10),t_2,1);
for i=1:t_1
d_1(i) = DD_1(i)*10^(-6);                                           % In order To Transform Particle Diameter in meter
V_1(i) = (4/3)*pi*(d_1(i)/2)^3;                                     % Volume of a particle
m_1(i) = qp_1*V_1(i);                                               % Mass of particle
Cc_1(i) = 1+((2*L/d_1(i))*(1.257+(0.4*exp((-1.1*d_1(i))/(2*L)))));
% Cunnigham correction factor for particle
RT_1(i) = (m_1(i)*Cc_1(i))/(3*pi*Vis*d_1(i));                       % Relaxation time of particle
end

for i=1:t_2
```

```
d_2(i) = DD_2(i)*10^(-6);              % In Order To Transform Droplet Diameter in meter
V_2(i) = (4/3)*pi*(d_2(i)/2)^3;     % Volume of a droplet
m_2(i) = qp_2*V_2(i);                % Mass of Droplet
Cc_2(i) = 1+((2*L/d_2(i))*(1.257+(0.4*exp((-1.1*d_2(i))/(2*L)))));
% Cunnigham correction factor for droplet
RT_2(i) = (m_2(i)*Cc_2(i))/(3*pi*Vis*d_2(i));              % Relaxation time of droplet
end

for j=1:t_1
for i= 1:50
a_1(j,i) = U*RT_1(j)*((i/RT_1(j))-1+exp(-i/RT_1(j)));          % X position of particle
b_1(j,i) = -((RT_1(j))^2)*g*((i/RT_1(j))-1+exp(-i/RT_1(j)));  % Y position of particle
end
alfa_1(j)=b_1(j,:)/a_1(j,:);                  % the ratio between X and Y path of particle
end

for j=1:t_2
for i= 1:50
a_2(j,i) = U*RT_2(j)*((i/RT_2(j))-1+exp(-i/RT_2(j)));          % X position of droplet
b_2(j,i) = -((RT_2(j))^2)*g*((i/RT_2(j))-1+exp(-i/RT_2(j)));  % Y position of droplet
end
alfa_2(j)=b_2(j,:)/a_2(j,:);                   % the ratio between X and Y path of particle
end
h = 150;                                          % in order to adjust the axis
[x,y,z] = sphere(50);
S_1 = floor(unifrnd(-100,100,t_1,3));
S_2 = floor(unifrnd(-100,100,t_2,3));
%S = randint(30,3,[-100,100]);            % an array that is randomly
set(gca,'nextplot','replacechildren');
for j=1:50                                       % for loop as 50 seconds
for i=1:t_1                                       % for loop in order to locate particles randomly
c(i) = surf (x*(DD_1(i))+S_1(i,1)+j,y*(DD_1(i))+S_1(i,2)+(alfa_1(i)*j),z*(DD_1(i))+S_1(i,3));
hold on
set (c,'edgelighting','gouraud','edgecolor',[0.3 0.3 0.3],'facelighting','gouraud','facecolor',[0.3 0.3 0.3]);
set(gcf,'DefaultAxesColorOrder',[1 0 0;0 1 0;0 0 1]);
axis ([-h h -h h -h h]);
axis off
end
```

```
for i=1:t_2                                    % for loop in order to locate droplet
randomly
s(i) = surf
(x*(DD_2(i))+S_2(i,1)+j,y*(DD_2(i))+S_2(i,2)+(alfa_2((i))*j),z*(DD_2(i))+S_
2(i,3));    hold on
set
(s,'edgelighting','gouraud','edgecolor','c','facelighting','gouraud','facecolor','c');

set(gcf,'DefaultAxesColorOrder',[1 0 0;0 1 0;0 0 1]);
axis ([-h h -h h -h h]);
axis off
end
light('Position',[0 0 1],'Style','infinite');
F(j)=getframe;                                  % in order to play as movie
hold off
end
mov = avifile('ilker.avi');
mov = addframe(mov,F);
mov = close(mov);
```

APPENDIX C

MATLAB CODE FOR COLLISION EFFICIENCY

```
T = input('ENTER THE TEMPERATURE (K) = ');                                  % Temperature
P = input('ENTER THE PRESSURE (atm) = ');                                   % Pressure
D_1 = input('ENTER THE PARTICLE DIAMETER (micron) = ');                     % Particle Diameter
D_2 = input('ENTER THE DROPLET DIAMETER (micron) = ');                      % Droplet Diameter
t_1 = input('ENTER THE NUMBER of PARTICLES = ');                            % Particle Number
t_2 = input('ENTER THE NUMBER of DROPLETS = ');                             % Droplet Number
qp_1 = input('ENTER THE PARTICLE DENSITY (kg/m^3) = ');                     % Particle Density
qp_2 = input('ENTER THE DROPLET DENSITY (kg/m^3) = ');                      % Droplet Density
VV = input('ENTER THE VISCOSITY OF FLUID X 10^7 (kg/m.s) = ');              % Viscosity of Fluid
U = input('ENTER THE UNIFORM FLUID VELOCITY (m/s) = ');
% Uniform Fluid Velocity
Vis = VV*10^(-7);                                                           % In Order To Transform Viscosity In kg\m.s
pr = P*101325;                                                              % In order To Transforn Pressure In bar
g = 9.8;                                                                    % Gravitational Acceleration
L = (23.1*T)/pr;                                                            % Molecular mean free path in gas (micron)
for r=1:100
FF=[]; KK=[]; HH= [];SD= [];JK= []; SLD=[]; JKL=[]; DD_1=[]; DD_2=[]; S_1=[]; S_2=[];
DD_1=normrnd(D_1,(D_1/10),t_1,1);                                           % Particle size distribution
DD_2=normrnd(D_2,(D_2/10),t_2,1);                                           % Droplet size distribution
for i=1:t_1
d_1(i) = DD_1(i)*10^(-6);                                                   % In order To Transform Particle Diameter in meter
V_1(i) = (4/3)*pi*(d_1(i)/2)^3;                                             % Volume of a particle
m_1(i) = qp_1*V_1(i);                                                       % Mass of particle
Cc_1(i) = 1+((2*L/DD_1(i))*(1.257+(0.4*exp((-1.1*DD_1(i))/(2*L)))));
% Cunnigham correction factor for particle
```

```
26.  RT_1(i) = (m_1(i)*Cc_1(i))/(3*pi*Vis*d_1(i));          % Relaxation time of
     particle
27.  end
28.  for i=1:t_2
29.  d_2(i) = DD_2(i)*10^(-6);                  % In Order To Transform Droplet
     Diameter in meter
30.  V_2(i) = (4/3)*pi*(d_2(i)/2)^3;          % Volume of a droplet
31.  m_2(i) = qp_2*V_2(i);                    % Mass of Droplet
32.  Cc_2(i) = 1+((2*L/DD_2(i))*(1.257+(0.4*exp((-1.1*DD_2(i))/(2*L)))));
33.  % Cunnigham correction factor for droplet
34.  RT_2(i) = (m_2(i)*Cc_2(i))/(3*pi*Vis*d_2(i));          % Relaxation time of
     droplet
35.  end
36.  for j=1:t_1
37.  for i= 1:10
38.  a_1(j,i) = U*RT_1(j)*((i/RT_1(j))-1+exp(-i/RT_1(j)));          % X position of
     particle
39.  b_1(j,i) = -((RT_1(j))^2)*g*((i/RT_1(j))-1+exp(-i/RT_1(j)));  % Y position of
     particle
40.  end
41.  alfa_1(j)=b_1(j,:)/a_1(j,:);                  % the ratio between X and Y
     path of particle
42.  end
43.  for j=1:t_2
44.  for i= 1:10
45.  a_2(j,i) = U*RT_2(j)*((i/RT_2(j))-1+exp(-i/RT_2(j)));          % X position of
     droplet
46.  b_2(j,i) = -((RT_2(j))^2)*g*((i/RT_2(j))-1+exp(-i/RT_2(j)));  % Y position of
     droplet
47.  end
48.  alfa_2(j)=b_2(j,:)/a_2(j,:);                % the ratio between X and Y path
     of droplet
49.  end
50.  h = 150;                                    % in order to adjust the axis
51.  [x,y,z] = sphere(50);
52.  S_1 = floor(unifrnd(-100,100,t_1,3));                % randomness of
     center of particles
53.  S_2 = floor(unifrnd(-100,100,t_2,3));                % randomness of
     center of droplets
54.  for i=1:t_1
55.  for j=1:10
56.  aa(i,j)=S_1(i,1)+j ;                        % X component of particle for all
     time
57.  bb(i,j)=S_1(i,2)+(alfa_1(i)*j) ;            % Y component of particle for all
     time
58.  cc(i,j)=S_1(i,3) ;                          % Z component of particle for all
     time
59.  end
60.  end
61.  for i=1:t_2
```

```
for j=1:10
AA(i,j)=S_2(i,1)+j ;                          % X component of droplet for all
time
BB(i,j)=S_2(i,2)+(alfa_2(i)*j) ;              % Y component of droplet for all
time
CC(i,j)=S_2(i,3) ;                            % Z component of droplet for all
time
end
end
for i=1:t_1
for j=1:t_2
for k=1:10                                    % distance between particle center and
droplet center
d(i,j,k)=((aa(i,k)-AA(j,k))^2+(bb(i,k)-BB(j,k))^2+(cc(i,k)-CC(j,k))^2)^(1/2);

if d(i,j,k)<((DD_1(i)+DD_2(j))/2)
FF=[FF;[i,j,k]];              % to check the distance for collision between particle
and droplet
end
end
end
end
if isempty(FF)
tcp(r)=0;
else
for i=1:t_1
KK(i,1)=1-all(FF(:,1)-i);
end
tcp(r) = sum(KK);             % number of captured particles
end
for i=1:((t_2)-1)
for j=(i+1):t_2
for k=1:10                 % distance between droplet centers
DDD(i,j,k)=((AA(i,k)-AA(j,k))^2+(BB(i,k)-BB(j,k))^2+(CC(i,k)-
CC(j,k))^2)^(1/2);
if DDD(i,j,k)<((DD_2(i)+DD_2(j))/2)
SD=[SD;[i,j,k]];                      % to check the distance for collision between
droplets
end
end
end
end
if isempty(SD)
ddc(r) =0;
else
for i=1:t_2
JK(i,1)=1-all(SD(:,1)-i);
end
ddc(r) = sum(JK);                                 % number of joined
droplets
```

```
103.  end
104.  for i=1:((t_1)-1)
105.  for j=(i+1):t_1
106.  for k=1:10                                        % distance between particle
      centers
107.  DKD(i,j,k)=((aa(i,k)-aa(j,k))^2+(bb(i,k)-bb(j,k))^2+(cc(i,k)-cc(j,k))^2)^(1/2);
108.  if DKD(i,j,k)<((DD_1(i)+DD_1(j))/2)
109.  SLD=[SLD;[i,j,k]];                  % to check the distance for collision between
      particles
110.  end
111.  end
112.  end
113.  end
114.  if isempty(SLD)
115.  ppc(r) =0;
116.  else
117.  for i=1:t_1
118.  JKL(i,1)=1-all(SLD(:,1)-i);
119.  end
120.  ppc(r) = sum(JKL);                                % number of
      agglomerated particles
121.  end
122.  eff(r)=tcp(r)/t_1;
123.  end
124.  rtrt = sum(eff)/100;
```